NASA-CR-205249

Geotail measurements compared with the motions of high-latitude auroral boundaries during two substorms

N. C. Maynard,[1] W. J. Burke,[2] G. M. Erickson,[3] M. Nakamura,[4] T. Mukai,[5] S. Kokubun,[6] T. Yamamoto,[7] B. Jacobsen,[8] A. Egeland,[8] J. C. Samson,[9] D. R. Weimer,[1] G. D. Reeves,[10] and H. Lühr [11,12]

Abstract. Geotail plasma and field measurements at -95 R_E are compared with extensive ground-based, near-Earth, and geosynchronous measurements to study relationships between auroral activity and magnetotail dynamics during the expansion phases of two substorms. The studied intervals are representative of intermittent, moderate activity. The behavior of the aurora and the observed effects at Geotail for both events are harmonized by the concept of the activation of near-Earth X lines (NEXL) after substorm onsets with subsequent discharges of one or more plasmoids down the magnetotail. The plasmoids must be viewed as three-dimensional structures which are spatially limited in the dawn-dusk direction. Also, reconnection at the NEXL must proceed at variable rates on closed magnetic field lines for significant times before beginning to reconnect lobe flux. This implies that the plasma sheet in the near-Earth magnetotail is relatively thick in comparison with an embedded current sheet and that both the NEXL and distant X line can be active simultaneously. Until reconnection at the NEXL engages lobe flux, the distant X line maintains control of the poleward auroral boundary. If the NEXL remains active after reaching the lobe, the auroral boundary can move poleward explosively. The dynamics of high-latitude aurora in the midnight region thus provides a means for monitoring these processes and indicating when significant lobe flux reconnects at the NEXL.

Introduction

Variations of the high-latitude ionosphere are regularly monitored by sensors at ground facilities and on satellites in low-Earth orbit rather than at their source regions in the magnetosphere. Thus it is useful to develop remote sensing techniques that improve understanding of magnetospheric processes through their ionospheric signatures. Such techniques have been developed and utilized to expand understanding of the dayside magnetosphere [*Newell et al.*, 1991; *Sandholt et al.*, 1990] and of substorm onset [*McPherron et al.*, 1973; *Elphinstone et al.*, 1995]. This study concerns the dynamics of the nightside, poleward boundary of the auroral oval. It is based on simultaneous ground and space measurements taken on January 14, 1994, during two substorms extending from 0600 to 0730 and from 1900 to 2200 UT. Throughout this day the Geotail satellite was in or near the distant plasma sheet where it observed substorm effects. Ground-based instrumentation of the Canadian Auroral Network for the OPEN Program Unified Study (CANOPUS) and International Monitor for Auroral Geomagnetic Effects (IMAGE) systems were operating in the midnight sector during the first and second substorms, respectively. Auxiliary measurements were also acquired by Defense Meteorological Satellite Program (DMSP) satellites in the ionosphere and Los Alamos National Laboratory (LANL) satellites at geosynchronous altitude.

The poleward boundary of the auroral oval lies at or near the boundary between open and closed magnetic field lines. Under conditions of steady convection the locations of this boundary should vary smoothly with the potential imposed across the polar cap by the solar

[1] Mission Research Corporation, Nashua, New Hampshire.
[2] Phillips Laboratory, Hansom Air Force Base, Massachusetts.
[3] Center for Space Physics, Boston University, Boston, Massachusetts.
[4] Department of Earth and Planetary Physics, University of Tokyo, Tokyo, Japan.
[5] Institute of Space and Astronautical Science, Sagamihara, Japan.
[6] Solar Terrestrial Environment Laboratory, Nagoya University, Toyokawa, Japan.
[7] Institute of Space and Astronautical Science, Kanagawa, Japan.
[8] Department of Physics, University of Oslo, Oslo, Norway.
[9] Department of Physics, Canadian Network for Space Research, University of Alberta, Edmonton, Alberta, Canada.
[10] Astrophysics and Radiation Measurements, Los Alamos National Laboratory, Los Alamos, New Mexico.
[11] Institut für Geophysik und Meteorologie, Technical University of Braunschweig, Germany.
[12] Now at Geo Forschungs Zentrum, Postdam, Germany.

Paper number 97JA00307.
0148-0227/97/97JA-00307$09.00

wind [*Siscoe*, 1982]. The basic assumption underlying this pedagogical model, namely, that steady convection is possible in a stably configured magnetosphere, may be incorrect [*Siscoe and Cummings*, 1969; *Erickson and Wolf*, 1980]. In ways still not fully understood, this deviation from stable equilibrium gives rise to magnetospheric substorms. Figure 1 of *Akasofu* [1964] illustrates the phenomenology of substorms in the nightside auroral oval. The onsets of substorms are marked by the brightening of the equatorwardmost auroral arc. This is followed by a rapid poleward expansion of the active region and the development of a bulge in the midnight sector. Thus the poleward boundary of auroral luminosity expands to high magnetic latitudes during the expansion phases and retreats equatorward during the recovery phases of substorms [*Craven and Frank*, 1987]. The poleward boundary is also marked by a pair of oppositely directed sheets of field-aligned currents. The more poleward current sheet is directed into the ionosphere [*Fujii et al.*, 1994]. Optical techniques have been developed to monitor the locations and motions of the poleward boundary of the auroral oval [*de la Beaujerdière et al.*, 1994]. From these the magnetotail reconnection rates have been estimated [*Blanchard et al.*, 1996].

The causal linkage between the magnetosphere and the high-latitude ionosphere during substorms has been a subject of long and fruitful research leading to the development of a model whose general features are widely accepted. Controversial details that continue to be debated have been reviewed by *Erickson* [1995]. After southward turnings of the interplanetary magnetic field (IMF), merging with the Earth's field is enhanced along the dayside magnetopause. Magnetic flux is transferred from the dayside magnetosphere to the nightside magnetotail. During the substorm growth phase, intensified and reconfigured magnetotail currents cause the shapes of field lines in the nightside, inner magnetosphere to stretch from dipolar to taillike [*Kaufmann*, 1987; *Baker and McPherron*, 1990]. Onset occurs on magnetic field lines that connect the inner edge of the plasma sheet with the ionosphere [*Maynard et al.*, 1996] and are frequently associated with northward turnings of the IMF [*Caan et al.*, 1975; *Lyons*, 1995]. They are marked by rapid dipolarization of near-Earth magnetic field lines and the development of westward electrojets spanning a few hours of local time in the midnight sector [*Singer et al.*, 1983]. This results from the partial diversion of cross-tail currents through the auroral ionosphere by means of filamentary field-aligned currents [*McPherron et al.*, 1973].

Hones [1977] outlined a global model of substorm dynamics that considers the consequences of a near-Earth X line (NEXL) forming as substorm activity expands. A byproduct magnetic O-type neutral line also forms and is expelled down the magnetotail as a plasmoid. Supportive evidence for the existence of substorm-related plasmoids in the magnetotail, as traveling compression regions, has been observed by IMP 8 [*Slavin et al.*, 1990] and ISEE 3 [*Slavin et al.*, 1993]. There is a nearly one-to-one correspondence between plasmoids observed in the far tail by ISEE 3 and earlier ground onsets [*Moldwin and Hughes*, 1993]. Since the launch of Geotail a number of particle and field detections of plasmoid signatures have been reported [*Frank et al.*, 1994; *Kawano et al.*, 1994; *Machida et al.*, 1994; *Nagai et al.*, 1994; *Nishida et al.*, 1994a, b]. Of particular interest for interpreting Geotail data in this paper are the heuristic model of *Machida et al.* [1994] for satellite encounters with tailward propagating plasmoids and the classification of variations in the magnetotail B_Z after substorm onsets developed by *Nagai et al.* [1994]. The concept of a quasi-stagnant plasmoid introduced by *Nishida et al.* [1986] provides a context for slower moving plasmoids propagating tailward inside a distant X line. This has recently been expanded to deduce simultaneously active near-Earth and distant X lines [see *Nishida et al.*, 1996; *Hoshino et al.*, 1996; *Kawano et al.*, 1996].

In the following sections we first briefly describe the ground- and space-based instrumentation which provide the data sources for our study and then present detailed descriptions of measurements taken on January 14, 1994, during two intervals of moderate substorm activity. In the discussion section we first compare the Geotail measurements in these weak-to-moderate events with predictions of the substorm plasmoid model [*Hones*, 1977]. The sequence of plasma flow directions observed during the first event indicates that Geotail exited a tailward moving plasmoid before its O line reached $X_{GSM} = -95$ R_E and entered a part of the magnetotail that was largely unaffected by substorm activity. Geotail returned to the plasmoid after its O line passed. The width of the plasmoid is limited in the Y_{GSM} direction. In the second substorm period, Geotail encountered signatures of a plasmoid with three embedded O lines. It was only after a third electrojet activation of this substorm that all previously closed field lines in the magnetotail were pinched off at the near-Earth neutral line. Subsequently, open flux from the lobe rapidly reconnected and then, as activity decreased, the X line moved tailward past Geotail. Poleward expansion of the auroral boundary occurs when open flux reconnects at a rate faster than steady state. Significant reconnection must have occurred on closed magnetic field lines within the plasma sheet prior to engaging reconnection of lobe field lines in the near-Earth region. When this new X line passed tailward of Geotail, the aurora had already begun to retreat equatorward, indicating that the period of rapid reconnection had ended.

Data Sources

January 14, 1994, was the fourth most disturbed day of the month, with K_P ranging from 3+ to 5. It was the continuation of an extended period of magnetic activity

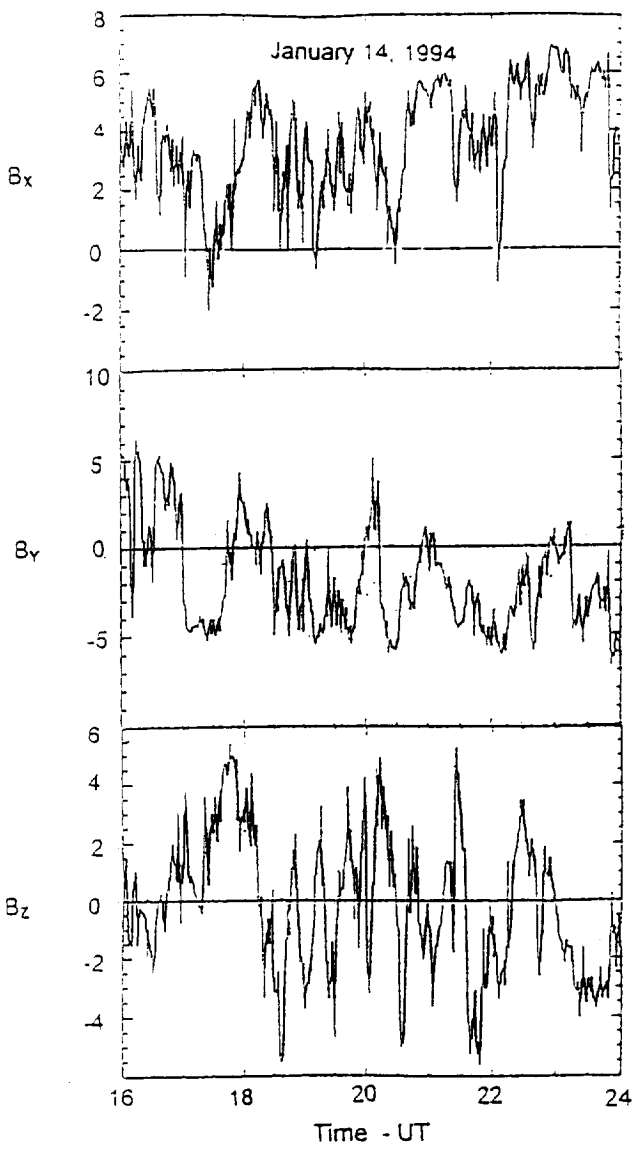

Figure 1. Three components of the interplanetary field, in geocentric solar-magnetospheric (GSM) coordidates, measured by IMP 8 during the last 8 hours of January 14, 1994.

that started in the middle of January 11 [*Nishida et al.*, 1995]. IMF data from the IMP 8 satellite have a gap during the first substorm interval. It is probable that IMF B_Y was negative, since it had that polarity both before and after the data gap. Figure 1 shows IMF measurements acquired during the last eight hours of the day. All three components were highly variable. This is characteristic of the entire day, including times prior to the first substorm.

Ground-based and satellite measurements of the high-latitude ionosphere are correlated with observations in the magnetotail from the Geotail spacecraft near X_{GSM} of -96 R_E. During the interval of the first substorm, ground magnetometer data and optical measurements came from CANOPUS stations in central Canada [*Rostoker et al.*, 1994]. Meridian scanning photometers were located at three CANOPUS stations along the magnetic meridian passing through Pinawa, Gillam, and Rankin Inlet. They are presented in a stacked-plot format to provide a history of the onset and poleward expansion of the substorm. Magnetometer measurements, taken along the same meridian, help identify the time of onset and locate the electrojet currents. During the second interval, ground data came from the IMAGE magnetometer chain [*Lühr et al.*, 1984], which extends from the Svalbard archipelago north of Norway into central Finland and from Tromsø in northern Norway. Meridian-scanning photometer and all-sky imager measurements were available from Ny Ålesund at Svalbard. The names and the geographic/geomagnetic locations of ground stations used in our study of the first and second substorm are given in Tables 1 and 2, respectively. In addition, supportive information is provided by energetic particle precipitation [*Hardy et al.*, 1984] and ion drift measurements [*Greenspan et al.*, 1986] from the DMSP F8, F10, and F11 satellites flying in circular, Sun-synchronous orbits at an altitude of 840 km. White-light optical images acquired by DMSP F10 have also been examined. Energetic ions and electrons from the LANL geosynchronous satellites 1990-095 and 1991-080 [*Belian et al.*, 1992] provided information on inner magnetosphere particle injections and constrained substorm onset definition.

The Geotail spacecraft is spin stabilized, completing 20 revolutions per minute. Its spin axis is maintained within 5° of perpendicular to the ecliptic plane. On January 14, 1994, Geotail was at apogee in the magnetotail near $X_{GSM} = -96$ R_E, $Y_{GSM} = 9$ R_E, and a few R_E south of the GSM equatorial plane. Allowing for the 4° aberration angle of the solar wind, Geotail was slightly to the eveningside of magnetic midnight during the periods of interest. Data from the magnetic field fluxgate (MGF) instrument [*Kokubun et al.*, 1994], the electric field detector (EFD) [*Tsuruda et al.*, 1994], and the low-energy particle (LEP) experiment [*Mukai et al.*, 1994] are used in this study. There are two triaxial fluxgate magnetometers on Geotail. They are located on a nonconducting mast at distances of 5.12 and 7.15 m from the spacecraft. Measurements for each component were made with 15 bit resolution in one of seven dynamic ranges from ±16 nT to ±65,536 nT at rates of 16 s^{-1}. These were averaged to produce one vector every 3 s. EFD measurements come from a double probe that uses spherical sensors. Each sphere is attached to and separated from the spacecraft body by a 50 m wire deployer. Data are sampled at rates of 32 or 64 s^{-1}. To avoid spurious effects due to asymmetric photoelectron currents, only data, acquired while the probes point in the ranges 60° to 120° and 240° to 300° with respect to the Sun, are used. These data are then fit to sinusoids to produce one measurement of the electric field components in the spin plane every 3 s. The LEP has three sensor components. Within the magnetosphere the energy-per-charge element is most useful.

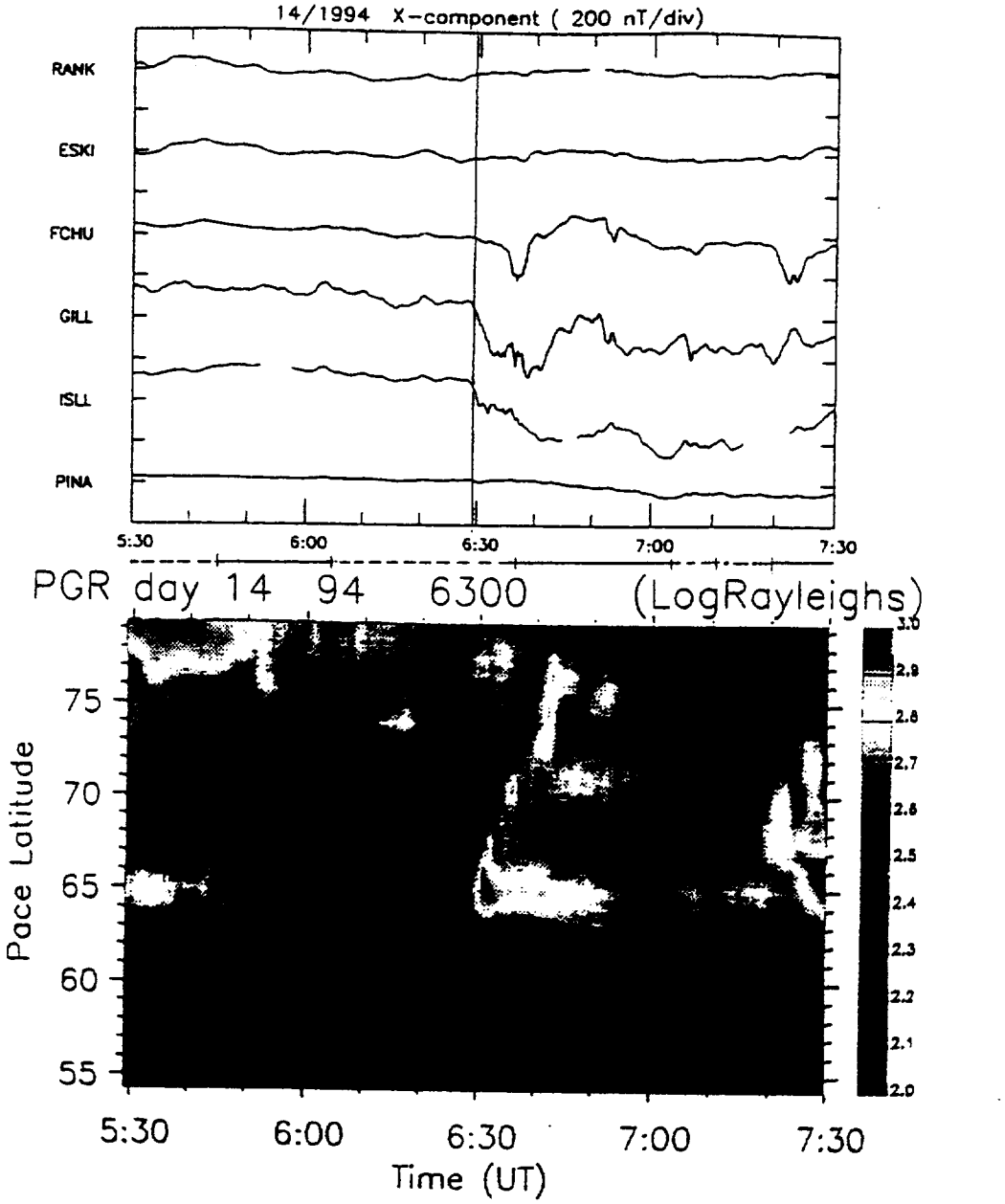

Plate 1. Magnetic and optical measurements from CANOPUS stations along the Rankin–Pinawa magnetic meridian between 0530 and 0730 UT on January 14, 1994. The 630.0 nm emissions were measured by three meridional scanning photometers at the Rankin Inlet, Gillam, and Pinawa stations. The intensity versus magnetic latitude spectrogram was compiled assuming an emission altitude of 230 km. The solid, dashed-dotted and dashed lines beneath the magnetograms represent different B_Z and V_X configurations encountered at Geotail and are described in the text.

It consists of two nested quadraspherical electrostatic analyzers. Directional differential fluxes for electrons and ions are sampled simultaneously in 32 energy steps and at seven spacecraft elevation angles. Electron energies are sampled from 8 eV to 38 keV. Ion energies per charge are measured from 32 eV/Q to 39 keV/Q.

First Substorm Interval: 0600 – 0730 UT

Plate 1 displays data from CANOPUS acquired during the first substorm event of January 14, 1994. The upper panels present the X component magnetic fields measured along the CANOPUS meridian chain (Table 1). To assist the reader in comparing ground measurements with those at Geotail, we have placed markings beneath the magnetograms of Plate 1, giving the relative polarities of the earthward-tailward V_X component of plasma flow and the north–south B_Z component of the magnetic field. Solid lines indicate periods when $B_Z > 0$ (northward) and $V_X < 0$ (tailward). Dotted-dashed lines indicate times when $B_Z < 0$ and $V_X < 0$; dashed lines indicate times when $B_Z > 0$ and $V_X > 0$. While

Table 1. Coordinates of CANOPUS Stations

Station	Abbreviation	GLAT	GLONG	ILAT	MLONG
Rankin Inlet	RANK	62.8°	267.9°	73.5°	328.9°
Eskimo Point	ESKI	61.1°	265.9°	71.8°	336.5°
Fort Churchill	FCHU	58.8°	265.9°	69.5°	336.7°
Gillam	GILL	56.4°	265.4°	67.2°	336.2°
Island Lake	ISLL	53.9°	265.3°	64.7°	336.4°
Pinawa	PINA	50.2°	263.9°	61.0°	335.1°

the instances $B_Z < 0$ and $V_X > 0$ have been observed by Geotail [*Nishida et al.*, 1995], they were not found during the periods of interest on January 14, 1994.

Substorm onset occurred at 0629 UT, just south of the Gillam station. It is marked by the start of negative bays at GILL and ISLL. This onset is also clearly seen as an intensification of 630.0 nm emissions, commencing at 0629 UT near 65° magnetic latitude (MLAT) then gradually stepping poleward. A significant enhancement of optical emissions occurred over Fort Churchill near 0636 UT. A decrease in the magnetic field X component also began simultaneously at that station. Optical activity progressed poleward to between 73° and 76° near 0641 UT. Note that after the initial activity the amplitudes of the magnetic deflections and the intensity of auroral emissions decreased slightly at the higher latitudes. However, optical and magnetic activity continued along the low-latitude border of the aurora near 65°. An intensification in the aurora near 75° occurred at 0650 UT. Shortly after 0710 UT the intensity of optical emissions at 74° dropped to background levels, characteristic of the polar cap. This indicates that the photometer scan crossed the open/closed field line and auroral oval/polar cap boundaries [*de la Beaujardiere et al.*, 1994; *Blanchard et al.*, 1996]. We conclude that the auroral brightening at 0641 UT (2340 magnetic local time (MLT)) marks the polar cap boundary as being near 79° MLAT, the northern most extent of optical

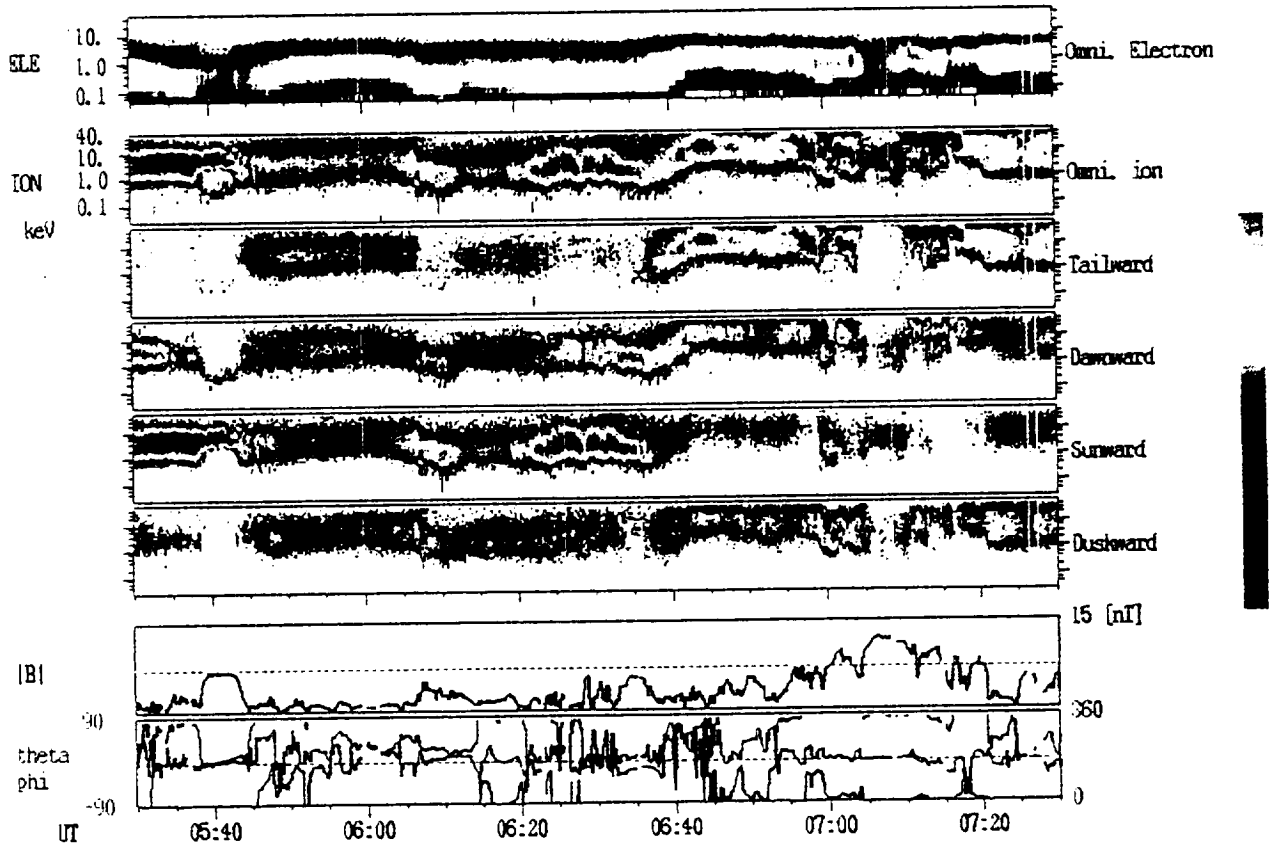

Plate 2. Measurements from the LEP instrument on Geotail spanning the first substorm interval in an energy-versus-time color spectrogram format. The top two plots give the omnidirectional, differential flux of electrons and ions. The lower spectrogram panels, from top to bottom give the directional differential flux of ions moving tailward, dawnward, earthward, and duskward, respectively. The magnitude of B and the polar (theta) and azimuthal (phi) angles of B are provided for reference in the bottom two line graphs.

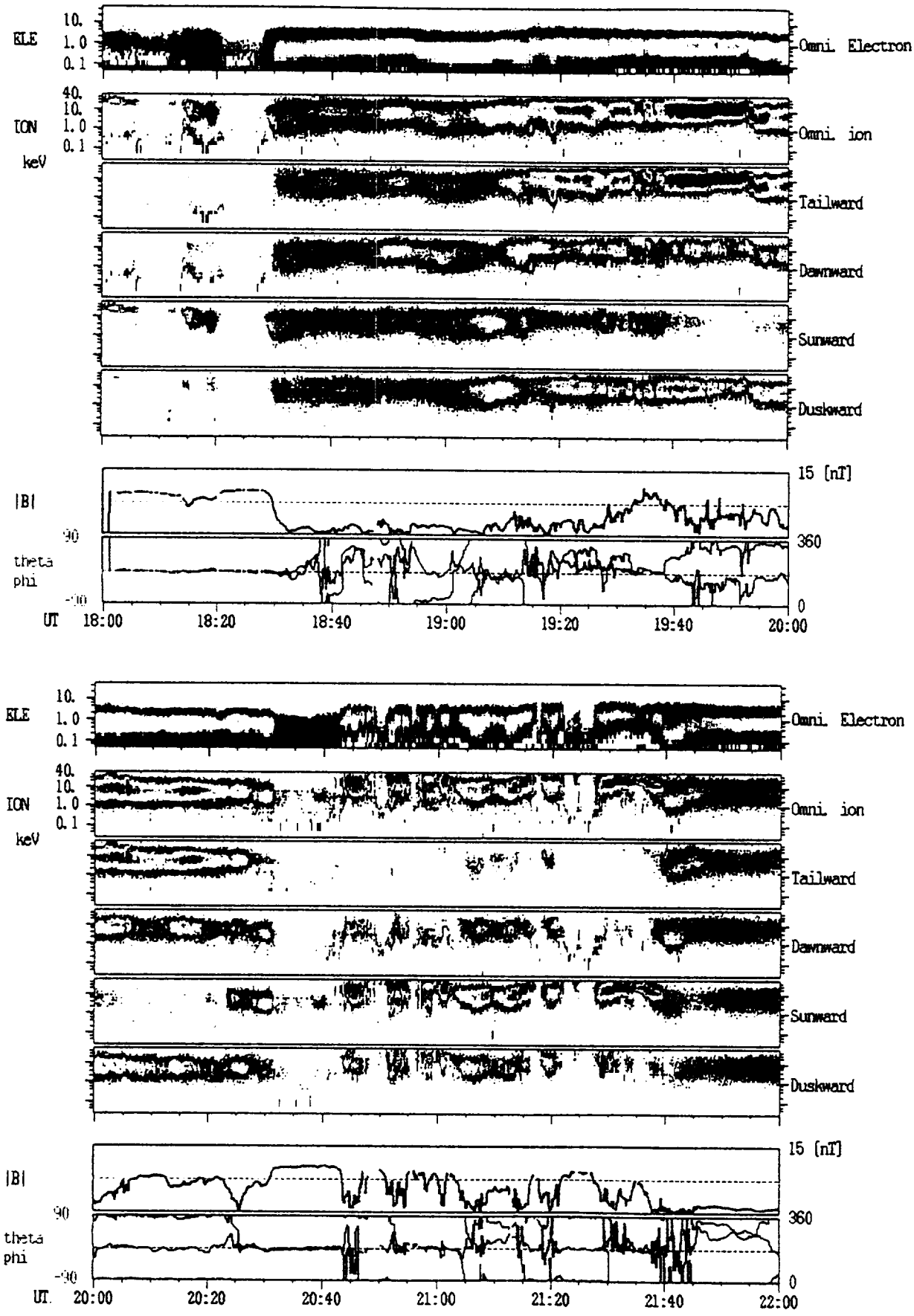

Plate 3. Measurements from the LEP instrument on Geotail spanning the second substorm interval in the same format as Plate 2.

Table 2. Coordinates of IMAGE Stations

Station	Abbreviation	GLAT	GLONG	MLAT	MLONG
Ny Ålesund	NAL	78.9°	11.9°	74.9°	114.3°
Longyearbyn	LYR	78.2°	15.8°	73.8°	115.3°
Hornesund	HOR	77.0°	15.6°	72.8°	113.1°
Hopen Island	HOP	76.5°	25.0°	71.4°	107.0°
Söröya	SOR	70.5°	22.2°	66.1°	110.3°
Masi	MAS	69.5°	23.7°	64.9°	110.6°
Muonio	MUO	68.0°	23.5°	63.5°	109.4°
Pello	PEL	66.9°	24.1°	62.4°	109.1°
Oulujärvi	OUJ	64.5°	27.2°	59.7°	110.2°

coverage. The boundary retreated equatorward in the subsequent minutes. The data in Plate 1 indicate that at ~0720 UT another activation of the substorm cycle initiated and lasted beyond the limits of our study.

A dawn-dusk pass of the DMSP F8 spacecraft (not shown), near the time of substorm onset, crossed the high-latitude, auroral boundary at ~78° MLAT and 1800 MLT. Rapid, antisunward plasma flows were detected just poleward of that boundary at 0631:30 UT. The boundary transition was sharp, with no particle precipitation on its poleward side. The polar cap potential measured during this pass was ~50 kV. The DMSP F11 spacecraft crossed nightside, southern high latitudes at 0656 UT. However, it did not fully enter the polar cap, detecting intense auroral precipitation up to its most poleward excursion of -73.1°MLAT at 2336 MLT. The location of the polar cap boundary and the most poleward precipitation observed by DMSP are consistent with the boundary of 630.0 nm emissions shown in Plate 1 for that time. We also note that the LANL satellite 1990-095 was near 0300 LT. At 0632 UT it detected an energy-dispersed electron injection, indicating that the satellite was located to the east of the substorm-activated region.

Figure 2 displays magnetic and electric field as well as as ion bulk flow components measured by Geotail during the first substorm event as functions of UT and the GSM locations of the satellite. Figure 2a shows the B_X component (GSM) of the magnetic field and the total magnitude of the magnetic field (dotted line). Figures 2b and 2c show B_Z and the Y_{GSM} component of the electric field, E_Y, respectively. Figures 2d - 2g show the velocity in the X_{GSM} direction V_X, the component of velocity parallel to the magnetic field (positive toward the Earth), as well as the X_{GSM} and Y_{GSM} components of the ion velocity perpendicular to the magnetic field, respectively. Substorm onset was at 0629 UT as determined from ground measurements. Note that at this time, and for most of the previous hour, the ion flow was earthward at Geotail and B_Z was positive. Plate 2 provides LEP measurements for the same period in an energy-versus-time spectrogram format. The top plot gives the omnidirectional, differential flux of electrons with energies between 8 eV and 38 keV. The lower plots represent directional differential fluxes of ions with energies per charge between 32 eV/Q and 39 keV/Q. As indicated on the plate, the look directions were selected to sample ions streaming in the tailward, dawnward, earthward, and duskward directions. With the exception of a brief excursion into the plasma sheet boundary layer (PSBL) at ~0540 UT, the spacecraft was in the plasma sheet prior to substorm onset, as indicated by low magnetic fields and elevated levels of particle fluxes. Thus the spacecraft was located in a region of closed magnetic field lines, with the distant X line tailward of its position during the growth and the early expansion phases of the substorm.

The ion flow turned tailward at 0637 UT (8 min after onset), becoming stronger and more energetic at 0642 UT. After a decrease a second enhancement was observed at about 0655 UT. During the period of strong tailward flow, B_Z was, with a few minor exceptions, northward. E_Y was negative, except when B_Z briefly changed sign, consistent with relatively steady tailward flow that lasted more than 20 min. The positive B_Z indicates that the satellite must have been on closed field lines while experiencing this tailward flow or was tailward of the O line within a plasmoid structure. Note that the beginning of the tailward flow at Geotail occurred ~8 min after substorm onset, approximately the time of auroral expansion to 70° MLAT (Plate 1). The increases in speed and intensity at 0642 and 0655 UT coincided with brightenings of the aurora in the vicinity of 75° MLAT.

At 0659 UT the ion flow turned sunward and field aligned as the spacecraft entered the PSBL. At this point, E_Y and B_Z were both positive, consistent with the observed earthward ion flow. The flow turned tailward as B_Z briefly reversed sign and then returned earthward with positive B_Z. During the second period of earthward flow, the plasma velocity in the X_{GSM} direction was field aligned. From about 0710 to 0720 UT, B_Z turned negative, and the plasma velocity became strongly tailward; E_Y remained positive. In this interval of B_Z polarity changes, V_Y was significant and positive (dawn-to-dusk).

Second Substorm Interval: 1900 – 2200 UT

The second event did not have a clean onset. Figure 1 shows that after a period of primarily northward IMF, B_Z turned southward near 1815 UT. Large-amplitude

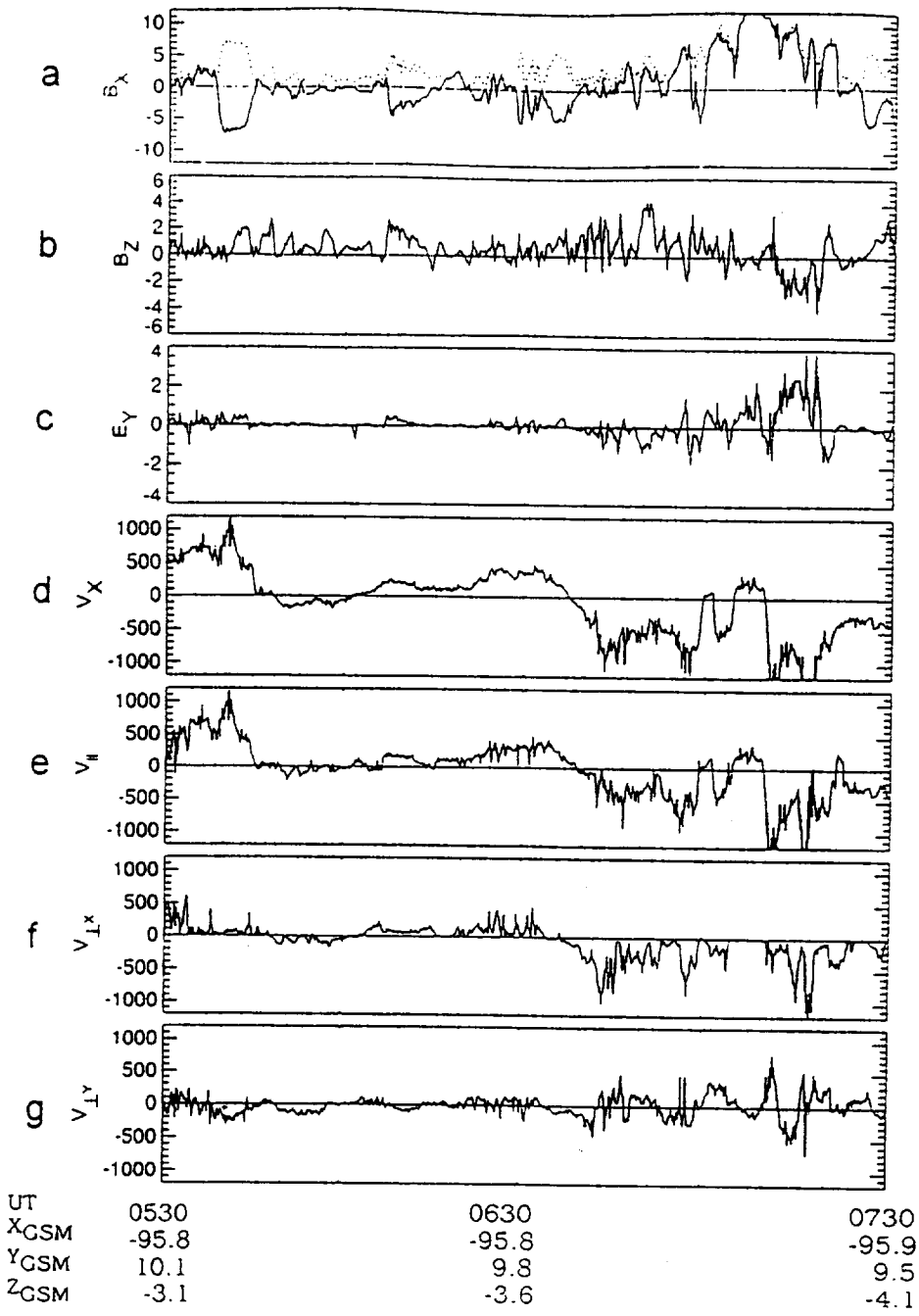

Figure 2. Magnetic field, electric field and ion drift velocities measured by the magnetic field fluxgate (MGF), electric field detector, (EFD), and low energy particle (LEP) instruments on Geotail between 0530 and 0730 UT on January 14, 1994. GSM components of vectors are presented. (a) The X and (b) Z of the magnetic field in nanoTeslas. (c) The dawn–dusk componet of the electric field in milliVolts/meter. (d) The earthward velocity component in kilometers per second. (e) The velocity components parallel to the Earth's magnetic field and (f) the earthward and (g) dawnward velocity components perpendicular to the magnetic field.

oscillations with periods between 27 and 31 min followed. Figure 3 gives the variations of the X component of the Earth's magnetic field observed along the IMAGE meridian chain of magnetometers. Activity initiated near the Söröya (SOR) and Masi (MAS) stations in northern Finland at ~1858 UT. It was also detected at Tromsø (not shown). Activity spread poleward, with a second initiation at 1925 UT. Table 2 indicates that there is a 5.3° magnetic latitude difference between the SOR and Hopen Island (HOP) stations. The station at Bear Island (BJN) which usually bridges that gap was not operational on that day. A third intensification be-

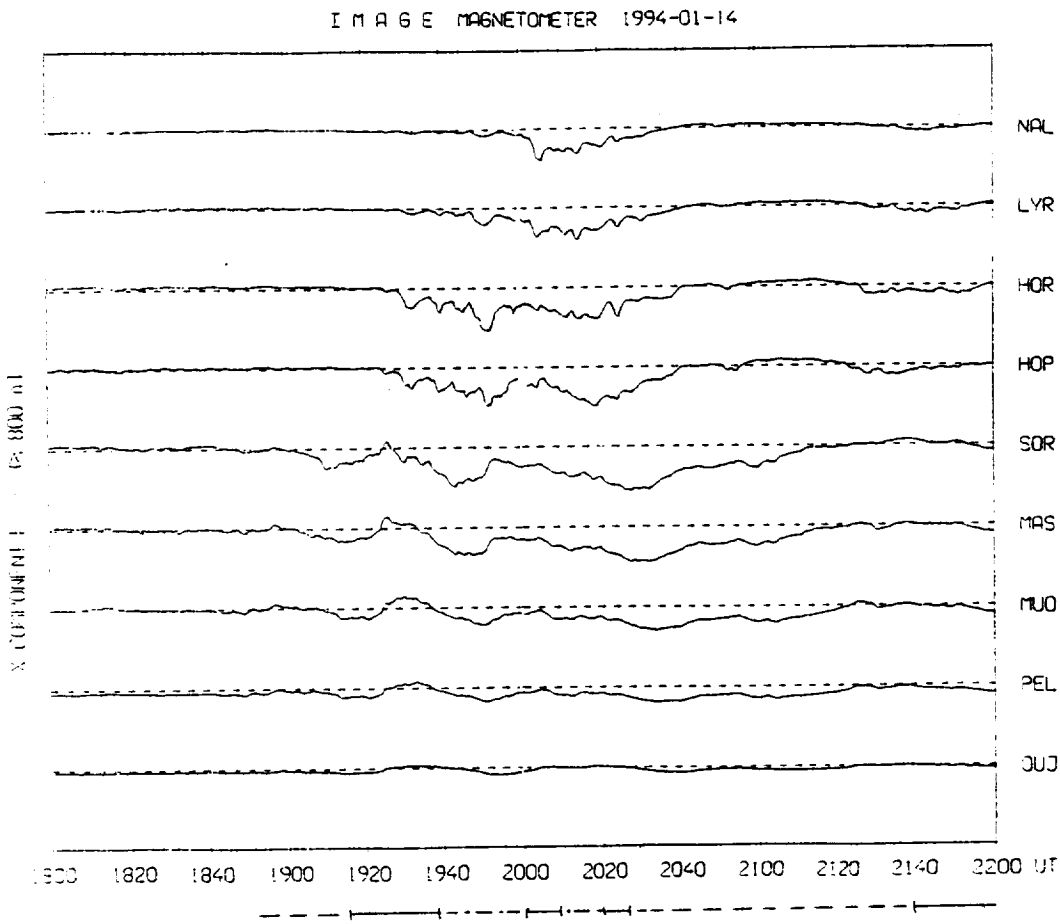

Figure 3. Variations of the X component of the Earth's magnetic field measured at stations along the IMAGE magnetometer chain during the second substorm interval.

gan near 1950 UT at the SOR and MAS stations and 2002 UT at HOP. A comparison with data in Figure 1 shows that that these activations occurred after northward turnings associated with the large oscillations of IMF B_Z. Exact relationships between solar wind/IMF variations and the substorm activations shown in Figure 3 are well outside the scope of this report.

Stack plots from the meridian scanning photometer measurements at Ny Ålesund of 557.7 nm emissions are presented in Figure 4. At 1925 UT the aurora appeared on the southern horizon of Ny Ålesund and gradually intensified, moving slightly poleward. After retreating near 1942 UT it continued poleward, expanding rapidly after 1955 UT. It crossed zenith at about 2000 UT and expanded to cover the visible sky with aurora until 2005 UT. All-sky images show that the decrease in the intensity of the emissions, observed between 2010 and 2020 UT in Figure 4, reflects a reduction in optical emissions over the entire sky. This occurred while IMF B_Z was northward for more than 10 min. At 2025 UT the aurora began to retreat southward, reaching and remaining near the horizon until 2140 UT when there was a brief, poleward excursion. We have also examined the meridian scanning photometer data from Longyearbyen located ~100 km south of Ny Ålesund (R. Smith, private communication, 1996), confirming the sequence of events at Ny Ålesund which are described above. To help in comparing ground and Geotail data, we have introduced the same symbolic markings that appear in Plate 1 beneath the magnetograms in Figure 3 and beside the photometer scans in Figure 4. The only additions are heavy lines to indicate times when, as discussed below, strong earthward enhancements of plasma flow were detected by Geotail.

Optical and particle data (not shown) reveal that DMSP F10 crossed the boundary of the polar cap into the auroral oval at 2028 UT (77° MLAT, 21.4 MLT). The satellite passed to the west of Ny Ålesund between Svalbard and Greenland. These DMSP measurements are consistent with our interpretation that the poleward auroral boundary at Ny Ålesund reflects the location of the open/closed boundary [*Blanchard et al.*, 1996]. Polar cap potentials measured by the DMSP satellites in this time interval were in the 50 to 70 kV range. The LANL satellite 1991-080 was in the midnight sector. It detected numerous, weak ion injections, the largest of which were at 1852, 1858, 1904, and 1909 UT. The most pronounced electron injections were detected at ~1927, 1941, 1951, and 2008 UT.

Figure 5 displays the Geotail data for this event in

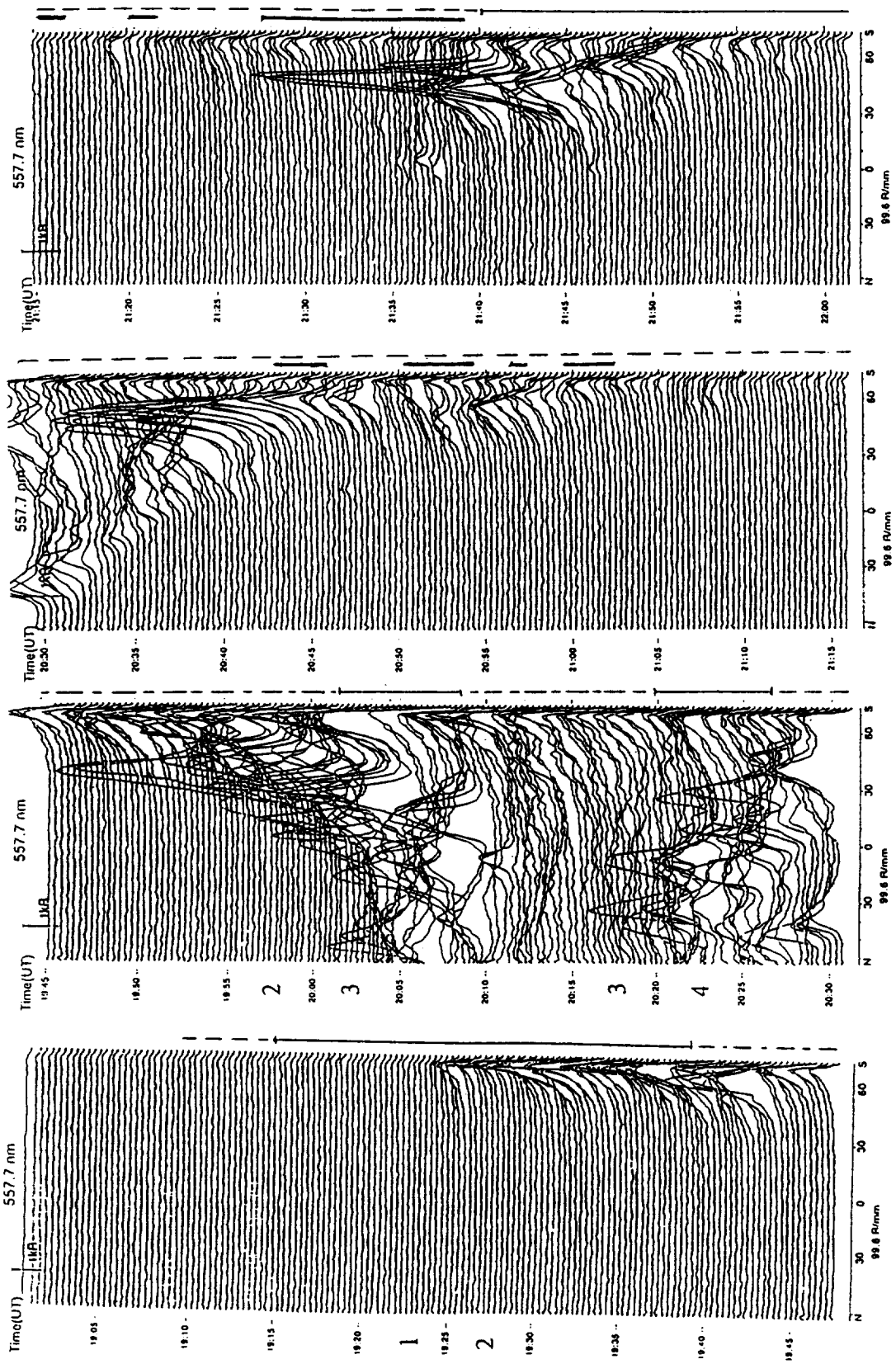

Figure 4. Stacked plots of magnetic meridional scanning photometer measurements from Ny Ålesund at 557.7 nm on January 14, 1994. The numbers 1 through 4 indicate the data segments described in the text. Solid, dashed-dotted and dashed lines beside the photometer sweeps represent different B_Z and V_X configurations encountered at Geotail in the same format as Plate 1. Heavy solid lines beside the photometer sweeps of segment 4 indicate times when intense, earthward plasma flows were detected by Geotail.

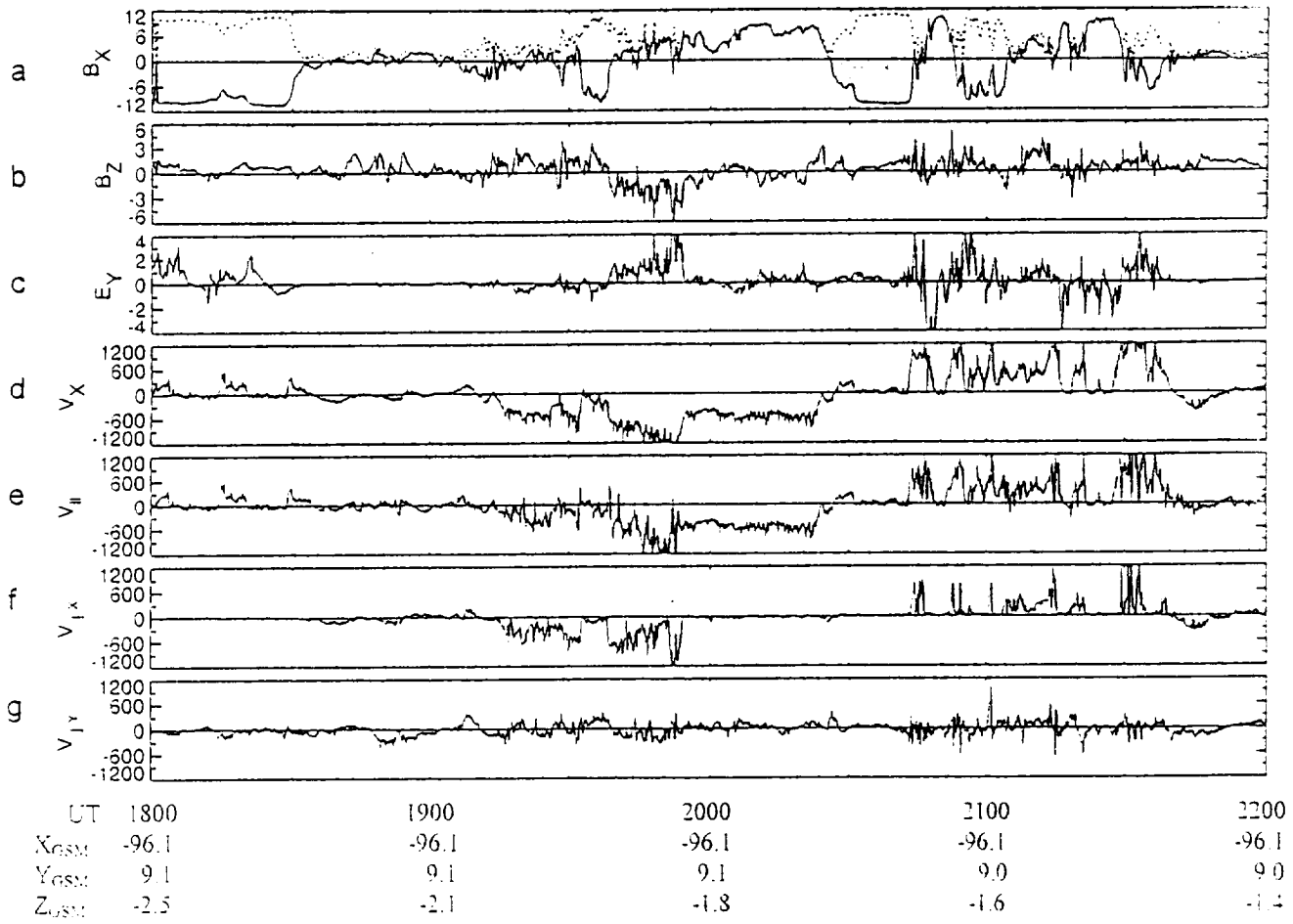

Figure 5. Magnetic field, electric field, and ion drift velocities measured by the MGF, EFD, and LEP instruments on Geotail between 1830 and 2230 UT on January 14, 1994, in the same format as Figure 2.

the same format as Figure 2. Omnidirectional electron fluxes and quadrature flows of ions are shown in Plate 3. To relate events at Geotail to ground observations and substorm phenomenology, we divide the Geotail data into four segments: (1) 1830 to 1925 UT, (2) 1925 to 2000 UT, (3) 2000 to 2021 UT, and (4) 2021 to 2150 UT.

In segment 1, Geotail entered the plasma sheet from the southern lobe at 1830 UT. The flow was weak and variable in direction until 1915 UT, when the plasma flow velocity increased to ~250 km s^{-1} and became predominantly in the $-X_{GSM}$ direction. B_Z remained positive, indicative of closed field lines, and E_Y became slightly negative (dusk to dawn). This initial effect at Geotail, relatable to ground activity, occurred ~17 min after the first electrojet activation when the average energies of electrons and ions rose to a few hundred eV and a few keV, respectively. These values are consistent with Geotail measurements in the plasma sheet.

In segment 2, B_Y increased in magnitude in the negative direction, becoming the dominant component. Between 1932 and 1938 UT, B_X became strongly negative, and the flow decreased to near zero as the satellite approached the southern PSBL. The primary flow was toward dusk but with regions of nearly isotropic fluxes (Plate 3). At 1938 UT the polarities of B_Z, E_Y, and V_Y reversed, B_X returned to near zero, and the plasma flow again became strongly tailward. B_Y was large, negative, and dominant in the next 3 min, after which it returned to near zero. This reversal in B_Z is different from the one in the previous substorm in that E_Y changed from negative to positive. It was positive on both sides of the B_Z reversal in the previous substorm period. There was no evidence of significant earthward flow. Between 1950 and 1955 UT, V_X peaked at >1000 km s^{-1}, and E_Y and B_Z also maximized. At 1955 UT these quantities quickly decreased with the flow returning to a nearly constant 500 km s^{-1} which was observed through most of segment 3.

In segment 3, B_X became large and positive, indicating that Geotail was in or near the northern PSBL. Since ion temperatures and densities remained high, the satellite did not enter the lobe. Data displayed in Plate 3 show that both the flow speed and the thermal spread of the ions decreased. Attention is directed to the B_Z and E_Y measurements in Figure 5 taken between 2000 and 2020 UT. For the first half of this period B_Z was positive and became negative for the second half. The

polarity of E_Y also changed from negative to positive consistent with continued tailward convection. These characteristics are similar to the polarity reversal at 1939 UT. Recall also that it was in this interval that the most poleward excursion of the aurora was observed at Ny Ålesund.

For segment 4, between 2021 UT and 2030 UT, B_Z was almost exclusively positive, and after a brief negative excursion E_Y remained positive. From 2028 UT until 2139 UT the dominant flow was earthward except for near-zero-velocity episodes when the satellite crossed into the southern lobe between 2031 and 2043 UT. Earthward flowing plasma and positive B_Z indicate that the satellite was again on closed field lines. Upon reentering the plasma sheet at 2043 UT, the ion fluxes detected by Geotail were variable. A series of earthward-flow intensifications appeared at 5 to 8 min intervals. The most severe velocity decreases occurred during brief excursions into the lobe from the PSBL. Thus, while the flow appears highly variable at the location of Geotail, it probably did not turn off between observations of fast flows. The several reversals of B_X during this period indicate that the tail was flapping with the satellite alternately in both the northern and southern PSBLs. The peaks in $V_{X\perp}$ occurred when the satellite was crossing the center of the plasma sheet. These flow enhancements continued until 2140 UT when the flow turned tailward for ~10 min. This time B_Z did not reverse, indicating that the tailward plasma flow occurred on closed magnetic field lines and was caused by processes happening nearer to the Earth than Geotail.

Discussion

Data presented in the previous sections can be used to study interactions of the magnetotail with the poleward portion of the auroral oval during substorms. In both cases the development of activity was measured by magnetometers arrayed along magnetic meridians in the midnight sector. In neither instance, however, did we observe an isolated substorm that developed steadily from a clear onset, through expansion, to maximum epoch and recovery. Multiple activations occurred in both periods. Given the variability of the IMF on January 14, 1994, this is not surprising. The activities did produce auroral substorm signatures, including rapid poleward expansions of aurora in the midnight sector, both within the auroral zone and at its poleward boundary. To uncover relationships between auroral activations and expansions and magnetospheric phenomena, it is useful to place the Geotail measurements in appropriate contexts of substorm-related events in the magnetotail and then check the consistency of interpretations against auroral signatures.

Most substorm models explain the observed growth-phase stretching of field lines as caused by intensified, plasma sheet currents and convection resulting from the enhanced transfer of flux from the day to the nightside of the magnetosphere until the start of the substorm expansion phase. *Hones* [1977] proposed that substorm expansion begins with the formation of a NEXL where magnetic reconnection proceeds on closed field lines, quickly cutting through to the lobes. This magnetic topology requires that neutral lines in the near tail form in pairs. Because of the configuration of nearby field lines, neutral lines where merging occurs are called X lines. Tailward of the X line, is a closed structure with an O-type neutral line near its center. Plasma trapped in the O configuration constitutes a plasmoid which convects down the tail away from the Earth. In the case illustrated by *Hones* [1977] all of the closed magnetic flux initially extending tailward of the NEXL becomes pinched off, and initially open field lines in the lobes of the tail reconnect at the NEXL. The rapid inclusion of newly reconnected flux in the magnetotail causes the closed field line region, and with it the NEXL, to expand tailward. After this the NEXL becomes the "distant" X line until the next substorm cycle.

For a satellite such as Geotail located in the distant plasma sheet, the signatures predicted by the NEXL model during a strong, isolated substorm are clear. (1) Some time after substorm onset, tailward plasma convection should be detected in a region with $B_Z > 0$ and $E_Y < 0$. (2) As the center of a plasmoid approaches the spacecraft, the polarities of B_Z and E_Y should reverse. (3) For a brief period after the X line passes the satellite, $B_Z > 0$ and $E_Y < 0$ should be detected. (4) As the magnetotail approaches equilibrium, both B_Z and E_Y should be positive as plasma convects earthward.

Another characteristic of plasma dynamics implicit in the NEXL model relates to the directions of field-aligned flows in the PSBL. *Schindler and Birn* [1987] showed that conservation of momentum requires flows of plasma along magnetic field lines near the separatrices associated with magnetic X lines. Thus, if an X line is located earthward/tailward of the observing spacecraft, plasma flow should be field-aligned and tailward/earthward in the boundary layer between the lobes and the plasma sheet [*Machida et al.*, 1994].

The presence of flux ropes make signatures of O line crossings more complex than in the simple picture of item 2. The relationship between plasmoids and flux ropes in the magnetotail is a much-discussed subject [*Slavin et al.*, 1995, and references therein]. Flux ropes result from field-aligned (force-free) currents that produce helical magnetic structures around high-field cores. *Slavin et al.* [1995] found that during ISEE 3 encounters with plasmoids, flux ropes were almost invariably embedded within the cores. The only possible encounter with the core of a plasmoid in the period studied here occurred near 1938 UT when B_Z reversed sign. An examination of B_Y measurements (not shown) at this time indicates that flux-rope signatures are indeed present. Flux-rope field lines connected at both ends to the Earth experience a drag from the ionosphere that might

explain the relatively slow speeds with which some large plasmoids are observed to propagate down the magnetotail [*Hughes and Sibeck*, 1987].

Nagai et al. [1994] examined B_Z responses in the magnetotail after 89 well-documented substorm onsets. They identify six categories. Bipolar responses indicate clear Geotail encounters with plasmoids in the plasma sheet. They are the most commonly observed signature in the range $-70 > X_{GSM} > -100$ R_E. The bipolar response in B_Z has an initial increase, a sharp reversal to a large negative peak, then a recovery to lesser negative values. The average duration between peaks was 4 min. The B_Z reversals are consistent with Geotail crossing O lines at the centers of plasmoids. The plasmoid may contain a flux rope at the center in which case B_Y and $|B|$ maximize. When Geotail was in the lobe of the magnetotail, the passage of a plasmoid was marked by traveling compression regions (type T). Less common responses included fluctuating B_Z (type F), often associated with multiple onset substorms, and situations when B_Z remained northward (type N) for extended periods after substorm onsets.

It is seen that the Geotail measurements reported here do not fit easily into the simple pictures of the *Hones* [1977] model. We contend that phenomenologically during the 0600 – 0730 UT interval Geotail encountered a type N structure. In the 1900 – 2200 UT interval, Geotail detected one type F and two modified bipolar signatures. In reality, the region of substorm engagement is finite in the Y_{GSM} direction [*Singer et al.*, 1983]. Also, not all substorms are isolated, strong, or even continuous. Moderate to weak events with multiple activations provide different perspectives for understanding substorm processes. In the following paragraphs we argue that the observed signatures reported herein are consistent with the basic concepts of *Hones* [1977] if we expand the picture to three dimensions and allow for a significant period of reconnection on closed magnetic field lines before the lobes are engaged at the NEXL. This implies a thick plasma sheet in the near-Earth region, perhaps with an embedded thin current sheet [see *Sergeev et al.*, 1993]. It also means that the distant X line can actively add flux to the closed field line region until reconnection at the NEXL breaks through to the lobes. This concept is implicit in the quasi-stagnant plasmoid observations of *Nishida et al.* [1996] and *Hoshino et al.* [1996] where two X lines can be active simultaneously.

Comparing Geotail data with auroral observations is difficult since it is impossible to know exactly which regions are magnetically conjugate. We submit the following postulates to constrain the interpretation of events at both locations. (1) Field lines in the nightside auroral oval with optical emissions are closed. (2) Electrons are accelerated near active X lines. Those with direct access to the ionosphere produce auroral emissions. (3) Merging of closed flux at a NEXL proceeds for a finite interval before engaging lobe field lines. (4) Until a NEXL engages lobe field lines, the motion of the poleward boundary of the auroral zone is controlled by the distant X line. (5) Activity at a NEXL does not necessarily correlate with the activity of a distant X line. (6) Onset brightening of the equatorwardmost arc is not directly caused by a NEXL.

Although the second disturbed interval appears phenomenologically more complex, it is easier to reconcile with predictions of the plasmoid model. We thus consider it before discussing the significance of measurements taken between 0600 and 0730 UT. The relationship between the observed auroral motions and intensifications with magnetotail dynamics are then explored.

Second Substorm Interval

Observations from the second substorm interval are quite complex. To help the reader grasp them as a whole, Figure 6 provides a summary timeline. Beginning at 1858 UT, ground magnetometers detected an activation and three distinct intensifications of the auroral electrojet. At the time of the first observed electrojet activation the LANL satellite 1991-080 at geostationary altitude in the midnight sector detected a small ion injection (the second in a series of small changes). The electrojet intensifications at 1925, 1950, and 2002 UT were followed by electron injections detected by the LANL satellite. In a previous study a few minutes delay was observed between dipolarization/ground onset and the arrival of injected particles at the altitude of the Combined Release/Radiation Effects Satellite (CRRES) (in the vicinity of geostationary altitude) [*Maynard et al.*, 1996]. We suggest that as conditions progressed from the initial ground activity at 1858 UT, a reconnection site developed. The relaxation of the electrojet at ~1909 UT indicates that reconnection at the newly created NEXL either slowed or stopped at this time. As a result of this activation, some field lines with O topologies are introduced into the magnetotail. These field lines and their associated plasma, plasmoid 1, should migrate tailward. This is consistent with the detection of tailward flowing plasma by Geotail with $B_Z > 0$ after 1915 UT and the reduction of flow at 1932 UT. The second intensification of the electrojet and particle injection corresponds to a reactivation of the reconnection site. This activity created more O-type field lines and plasmoid 2. Note that plasmoid 2 encompasses plasmoid 1 since no lobe field lines have yet reconnected. Plasmoid 2 is marked by the passage of an O line at 1938 UT and the reduction in flow at 1955 UT. Once more, however, reconnection then either slowed or stopped. It was only during the third activation, beginning at ~1950 UT, that reconnection at a NEXL engaged previously open flux. This was followed by the passage of the O line of plasmoid 3 at 2006 UT and the X line at 2021 UT. We return to this point in the discussion of auroral boundary dynamics.

Figure 7 sketches the cycle of events as a sequence of

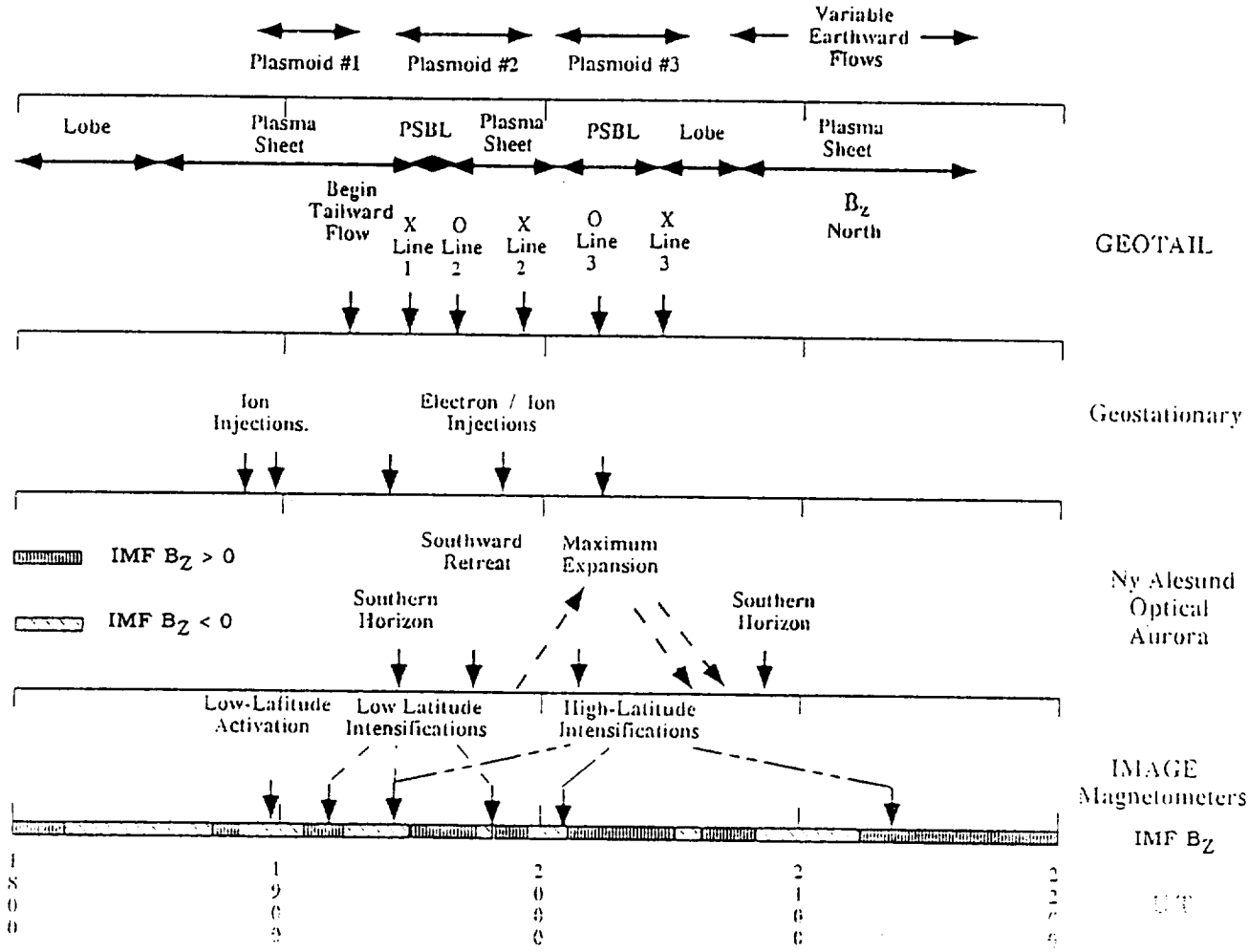

Figure 6. Summary timeline of observations during the second substorm interval of January 14, 1994.

magnetotail "states" during the four segments of this substorm interval. Prior to 1900 UT, convection in the plasma sheet near -96 R_E is earthward under the influence of a distant X line. Soon after this time a small plasmoid forms and moves tailward. The first sign of its existence appears at 96 R_E in the form of a reversal of V_X and E_Y, with B_Z remaining northward. In the second segment the ion flow remained tailward as the enlarged plasmoid 2 approached and moved past Geotail. The associated O line crossed the location of Geotail at 1938 UT. In segment 3 all of the initially closed field lines become pinched off, and the reconnection of open flux proceeds. As this third plasmoid, 3, convected downtail, Geotail moved into the PSBL where it could not fully encounter the O line typology. It did, however, detect the telltale signature of its passage in the bipolar responses of B_Z and E_Y. The reduction in velocity near 2025 UT marked the passage of the plasmoid. Geotail then moved into the southern lobe of the tail. When it reentered the plasma sheet, B_Z, E_Y, and V_X were again positive, consistent with the X line being tailward of its location. The enhancements in the earthward flow of energetic ions after this time are consistent with an active X line being located tailward of the satellite.

First Substorm Interval

Figure 8 gives a timeline overview of ground and space observations during the first substorm interval. Onset at 0629 UT was marked by an activation of the electrojet and a brightening of aurora at 65° invariant latitude (ILAT). The LANL satellite 1990-095, ~3 hours to the east of midnight, observed an energy-dispersed electron injection beginning at ~0632 UT. These data indicate that a dipolarization of the Earth's magnetic field occurred in the midnight sector.

The question arises regarding when a NEXL formed and a plasmoid propagated down the magnetotail. A schematic representation of a scenario that reconciles NEXL model predictions with Geotail observations is given in Figure 9. Figure 9a shows an equatorial-plane projection of the quiet time magnetotail with a distant X line. Convection is earthward/tailward on the earthward/tailward sides of the X line. Figure 9b indicates the changed situation after the time of onset when the NEXL X_1 forms. Figure 9c shows a plasmoid with a finite size in the Y_{GSM} direction after it has propagated to the vicinity of Geotail. The model predicts that Geotail should first detect tailward flowing, plasma sheet ions with $B_Z > 0$. From about 0638 to 0700 UT this

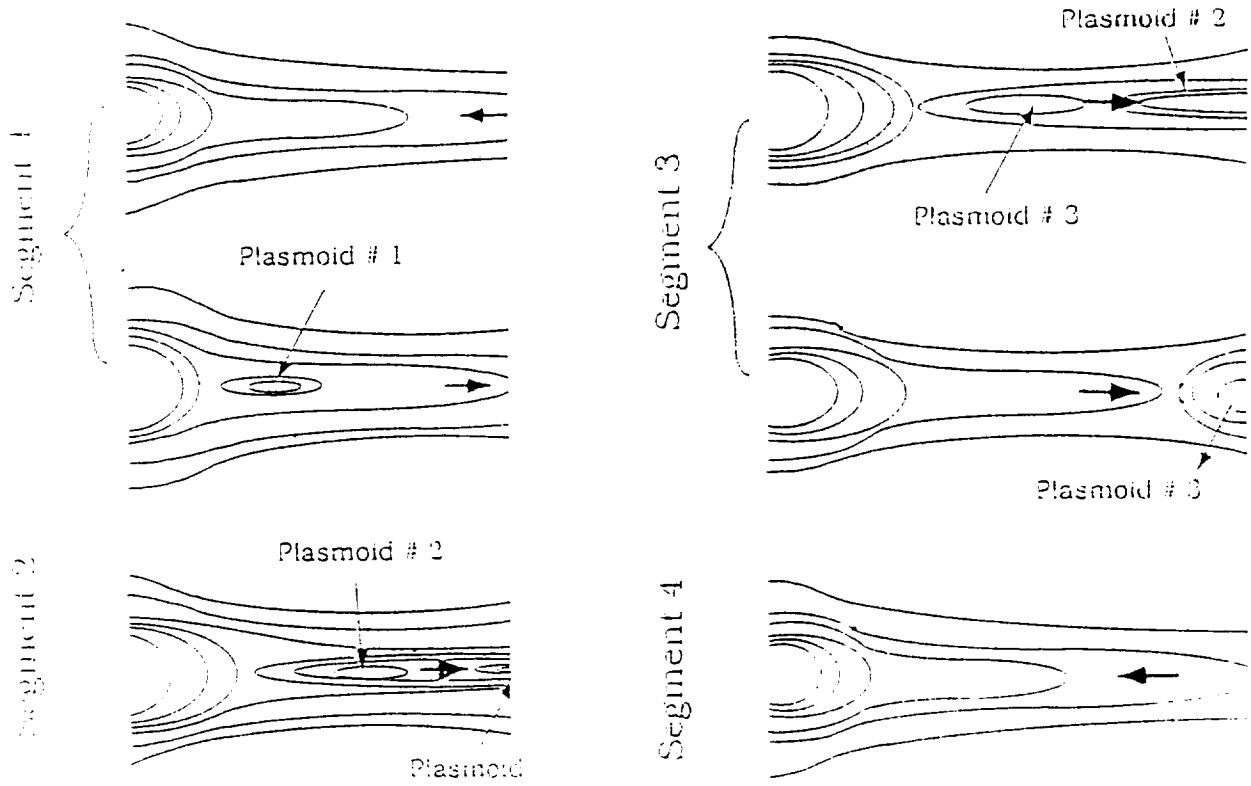

Figure 7. Schematic representation of magnetotail dynamics during the second substorm interval of January 14, 1994. The various diagrams show meridional cuts of the magnetotail appropriate for the different time segments defined in the text.

was true. However, instead of observing a reversal in the polarity of B_Z, Geotail moved into a portion of the PSBL with earthward ion flow. At 0711 UT, V_X became strongly tailward and $B_Z < 0$. At 0718 UT, B_Z turned northward, but the flow of plasma remained tailward.

Despite apparent difficulties the Geotail measurements are not inconsistent with NEXL generated plasmoid predictions of the *Hones* [1977] model. Critical for this interpretation is the observation of earthward flowing ions in the PSBL after 0700 UT. This can only mean that Geotail was temporarily on field lines whose dynamics were controlled by remnants of the distant X line. Recall that *Singer et al.* [1983] found that outside of a limited region in local time, field lines remained taillike after substorm onset. Thus a NEXL and its associated plasmoid are of limited Y_{GSM} extent. We also note that *Kivelson et al.* [1993] and *Angelopoulos et al.* [1996] postulated that plasmoids must have limited extent in the dawn-dusk direction in order to explain the lack of observation of a plasmoid from specific identified substorms. This case provides observational evidence of those conjectures.

As suggested by the Geotail "trajectory" in Figure 9c, the satellite exited a tailward moving plasmoid across its dawnside border. At a distance of 96 R_E the magnetotail moves by ~1.5 R_E for every 1° change in the solar wind direction. When Geotail returned to a region of plasma sheet fluxes at 0711 UT, both B_Z and V_X were negative. There are only two possible interpretations of this observation. Geotail either crossed the distant X line or reentered the plasmoid on the earthward side of its O line. Particle measurements shown in Plates 2 and 3 suggest that the latter interpretation is more plausible. In Plate 2 the earthward flowing ions in the PSBL (0700 – 0705 UT) had energies centered at a few hundred eV. During the $B_Z < 0$ interval the central energies of the tailward moving ions were >10 keV. They strongly resemble the ion fluxes detected from 1940 to 1952 UT (Plate 3) in the southward B_Z portion of plasmoid 2, discussed above. For the first interpretation to be correct it is necessary to postulate that the distant X line underwent a sudden activation and moved earthward. However, Plate 1 shows neither enhanced emissions nor new magnetic deflections near the auroral oval's poleward boundary at that time. Rather, the polarity reversal of B_Z at 0718 UT, with $B_X > 0$, indicates that Geotail returned to the plasmoid earthward of the O line. The X line passed the satellite near 0720 UT when B_Z again turned positive. The persistence of tailward flow after the passage of the X line suggests that a second, near-Earth X line X_2 formed near the time of the second activation (0720 UT) of the electrojet at Churchill.

Auroral Boundary Dynamics

The Geotail measurements provide clues for understanding auroral signatures during substorms just as those auroral signatures constrain our interpretation of Geotail signatures. The observed magnetotail dynamics seen at Geotail have been interpreted within the context

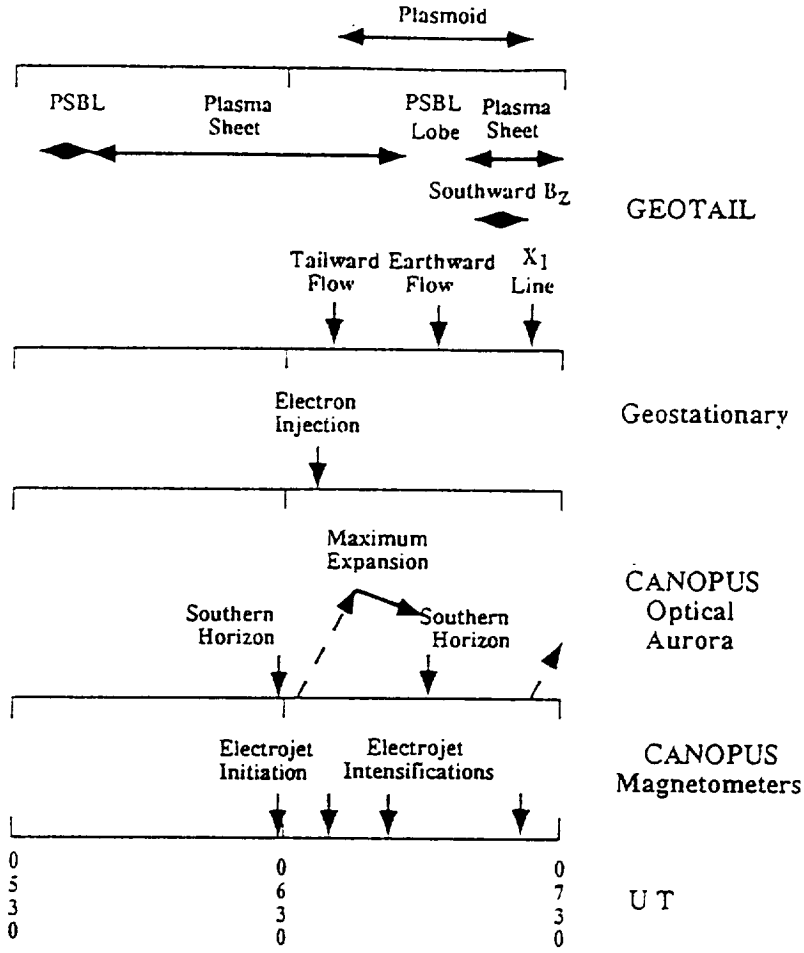

Figure 8. Summary timeline of observations during the first substorm interval of January 14, 1994.

of NEXL-generated plasmoids. We have deduced that during the second substorm interval, closed flux did not completely pinch off at the NEXL until the third electrojet activation. Afterward, open flux reconnected at the NEXL, activity diminished, and the X line eventually passed tailward of Geotail. In the first substorm case, Geotail moved outside and then back into a plasmoid that was spatially limited in the Y_{GSM} direction. The poleward boundary moved equatorward during this whole process. The following harmonizes these conclusions with the auroral observations.

Consider first some consequences in the auroral ionosphere of merging of lobe flux at an X line. We assume that the energized electrons responsible for the observed auroral emissions move along closed magnetic field lines. In the midnight sector at high latitudes the electric field causes the feet of these field lines to convect with an equatorward component of drift. A typical magnitude for this component is $\sim$1 km s^{-1}. In steady state flow the boundary between open and closed field lines in the auroral ionosphere should be stationary. Reconnection proceeds at a rate such that the inflow of open field lines to the boundary exactly matches the outflow of newly closed field lines. If a NEXL becomes active on closed magnetic field lines, the particles accelerated there produce auroral signatures. Until the last closed field line pinches off, auroral emissions are confined to latitudes equatorward of the mapping of the distant X line. As merging of closed flux at the NEXL proceeds, then electrons accelerated in the process acquire access to the auroral ionosphere at progressively higher latitudes. During this time, however, the distant X line still controls the motion of the poleward auroral boundary, and closed flux can be added or not as indicated by the boundary motion. Rapid poleward movement of bright aurora inside the poleward boundary indicates rapid reconnection at the NEXL. Rapid poleward movement of the poleward boundary indicates rapid reconnection of lobe flux, most likely at the NEXL.

Plate 1 shows that auroral emissions brightened at 65° at the time of onset (0629 UT). In the following 12 min the bright aurora expanded to 76°, a distance of $\sim$1200 km, and approached the poleward boundary of the oval. We believe that the 0636 UT auroral enhancement at Churchill (69.5°) was related to the activation of NEXL 1. Note that there are no emissions at this latitude prior to that activation, including the time of substorm onset, which places NEXL activation after

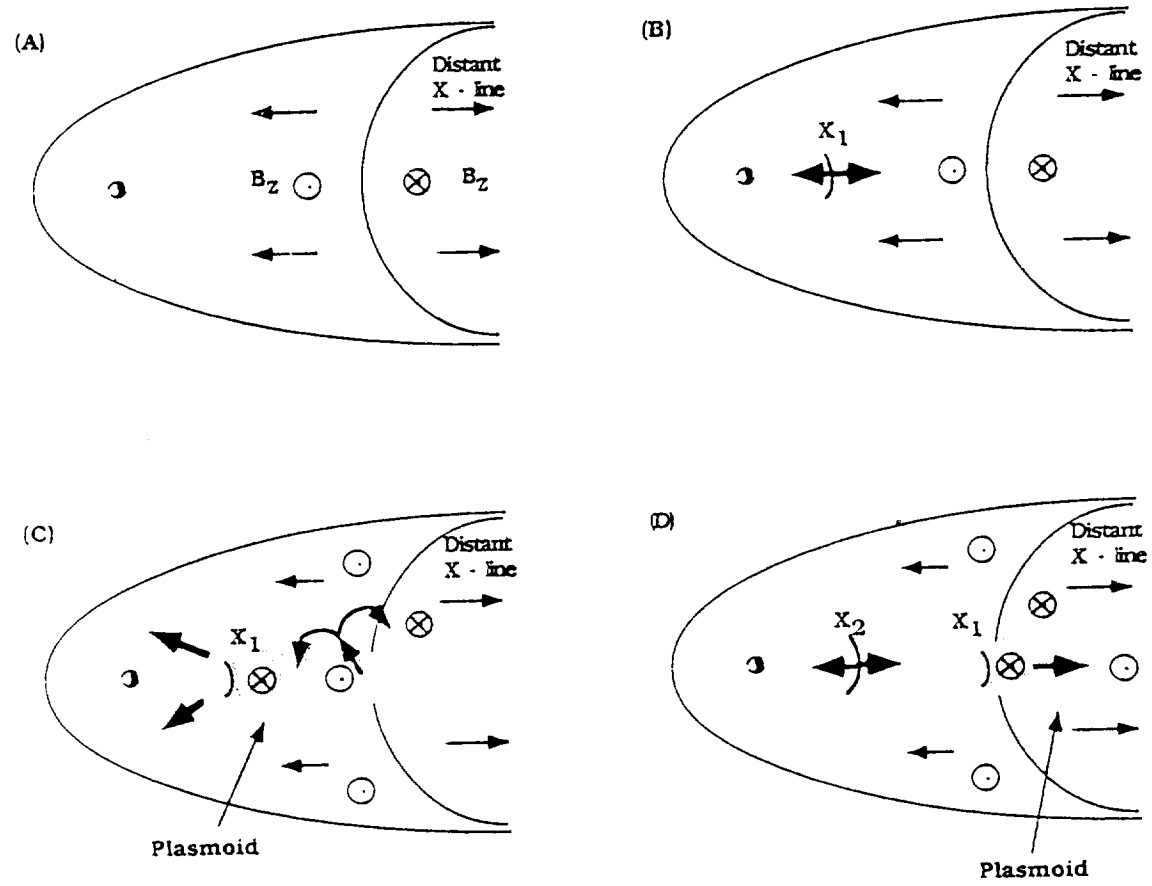

Figure 9. Schematic representation of magnetotail dynamics during the first substorm interval of January 14, 1994. Equatorial plane projections of the magnetotail appropriate for (a) presubstorm period, (b) substorm onset, (c) the period near 0700 UT when Geotail entered the plasma sheet boundary layer, and (d) the last electrojet activation of the interval are shown. The polarities of B_Z in the different regions are indicated.

onset as determined by ground magnetograms and enhanced aurora at the lower border. During the expansion phase the poleward boundary steadily retreated equatorward while the active aurora expanded poleward. This poleward expanding auroral activity was totally on the closed field lines. Note that the poleward auroral boundary retreated equatorward throughout the expansion phase, indicating that the distant X line controlled lobe flux reconnection, but reconnection was at a slower rate than flux transport from the dayside. On the basis of the poleward migration of the active aurora to the poleward boundary we conclude that reconnection progressed to the lobe magnetic field lines but did not engage the lobe until after 0720 UT when the poleward boundary started moving poleward. The lack of an enhancement in auroral emissions as the poleward boundary moved equatorward near 0711 UT is consistent with our suggestion that the distant X line did not move earthward; rather, Geotail exited and reentered a plasmoid that was spatially restricted in local time.

The second interval was marked by three electrojet intensifications at 1858, 1925, and 1950 UT. The first produced no optical emissions in the Ny Ålesund field of view and only a very small emission at the edge of the field of view 100 km to the south (at Longyearbyen). The second intensification was accompanied by ~1 kR emissions from near the southern horizon at Ny Ålesund. Only after the intensification of 1950 UT did the aurora rapidly expand poleward across the sky. We associate the poleward movement with rapid reconnection of lobe field lines at the NEXL. As the rate of reconnection slowed, the NEXL moved down the tail, and the poleward auroral boundary retreated equatorward. Open flux was being added faster on the dayside than it was being reconnected on the nightside. That the X line continued to be active after its passage beyond Geotail is evidenced by enhanced earthward flows. Brightenings in the aurora are seen at the poleward boundary during the equatorward retreat. Some of these produce equatorward moving auroral forms. It is not possible to correlate these events directly with individual enhancements of earthward flows at Geotail; however, we believe that these phenomena may be related, although not on a one-to-one basis. The flow enhancements are both spatially and temporally variable.

Our two events are examples of magnetotails with multiple, active X lines. *Hoshino et al.* [1996] reached

a similar conclusion for an event occurring 3 days after our events. The concept of a quasi-stagnant plasmoid [*Nishida et al.*, 1986] was originally postulated for slowly moving plasmoids, and it was described as a preexpansion phenomena. The slow moving plasmoid was often followed by a fast moving plasmoid associated with a substorm expansion phase. Our events occur after the onset of ionospheric substorm activity. The quasi-stagnant event seen by *Kawano et al.* [1996] was also after a ground onset, and it was also followed by a fast moving plasmoid associated with a later onset. Our results, complemented by those of *Hoshino et al.* [1996] and *Kawano et al.* [1996], show that moderate and variable substorm activity can create slow tailward moving plasmoids that are within closed field lines being added by an active distant X line.

Energization from the Reconnection Process

During the first event and the first two activations of the second event, tailward velocities observed at Geotail increased with time. This may reflect the location of the NEXL relative to the lobe. The outflow from the X line occurs at some fraction of the Alfvén velocity in the inflow region [*Vasyliunas*, 1975]. The Alfvén velocity is smallest in the center of the plasma sheet and increases toward the PSBL. Thus we expect to detect increasing velocities outflowing from reconnection sites as merging progresses toward the lobes. If merging is intermittent, if the distance to lobe magnetic field lines in the near tail is large, and/or if closed field lines are being added by the distant X line almost as fast as field lines are merged by the NEXL, that velocity increase could be over a significant interval of time (e.g., Figure 5 between 1915 and 1955 UT). Consistent with our interpretation that lobe flux reconnected at the NEXL during the third activation (~1950 UT), the velocity measured by Geotail during the encounter with plasmoid 3 remained constant with time. We note a similar increasing trend in V_X in Figure 1 of *Hoshino et al.* [1996]. They deduced that two X lines were simultaneously active for that event, although they did not comment on the trend or the cause.

A related effect has been found by *Baumjohann et al.* [1996] in a superposed epoch analysis of substorm effects between 10 and 19 R_E inside the NEXL region. For substorms which are not magnetic storm associated, the average earthward ion bulk speed gradually increases for the first 45 min after onset, while for storm associated substorms, it peaks much more quickly. They conclude that it is unlikely that lobe magnetic field lines are reconnected in the nonstorm case, and since the average ion temperature is similar in each category, the heating of plasma sheet ions is governed by reconnection on closed plasma sheet lines rather than open lobe field lines in the storm-related substorms. Our results suggest that the dynamics of the nightside aurora, especially at and near the poleward boundary, provide a means to monitor if, how quickly, and to what extent the reconnection process engages the lobes.

Conclusions

Activity observed in these two events provides insight into the behavior of substorms and the magnetotail under variably driven conditions. These may be more representative of day-to-day routine occurrences than commonly studied isolated or large events. On the basis of the data comparisons and the premises for interpretation stated above, we conclude the following:

1. Reconnection of closed flux at a NEXL can occur either continuously or intermittently for significant time intervals. During the first event near-Earth reconnection reached the lobes in about 15 min. In the second event it took three activations and more than 40 min to engage lobe field lines.

2. Plasmoids are three-dimensional structures, which are spatially limited in the Y_{GSM} direction. This is necessary to explain Geotail magnetic field and ion flow measurements during the first event. It is also consistent with near-Earth observations showing that the region of dipolarization is confined to a few hours in magnetic local time [*Singer et al.*, 1983].

3. Since the poleward boundary of the aurora delineates the last closed field line between the lobe and the PSBL, its motions are controlled by balances between the rates of flux transport from the dayside and reconnection in the magnetotail. Rapid poleward motions of that boundary, as observed after the third activation of event 2, indicate high rates of reconnection of lobe flux, most likely at a NEXL.

4. Equatorward motions of the poleward, auroral boundary during periods of increased magnetic activity are consistent with residual lobe-flux reconnection by the distant X line. Photometer measurements in Plate 1 indicate that at such times, NEXL activity is on closed magnetic field lines.

5. Multiple activations of a near-Earth reconnection site can result in multiple NEXLs before reconnecting lobe flux. Reconnection at the distant X line can continue to supply energy and closed flux to the system and prolong the time required before the NEXL begins reconnecting lobe flux.

6. The long duration of NEXL activation on closed magnetic field lines suggests that the plasma sheet was relatively thick. It may have had embedded within it a thin current sheet usually associated with NEXL activation.

7. Optical and Geotail observations during event 1 provide evidence that the onset of the reconnection at the NEXL occurs after the beginning of activity detected by ground magnetometers.

This study suggests that ionospheric variations can be used to monitor activity in the magnetotail. The motions of the auroral oval's poleward boundary in the midnight sector reflect the dynamic balance between flux transport from the dayside and reconnection in the magnetotail. They also serve as proxies for indicating when near Earth neutral lines assume control of lobe flux reconnection.

Acknowledgments. This work was a collaborative effort spawned from the NSF GEM Workshops and common data collection intervals. A. Nishida was instrumental in establishing the original collaboration. O. de la Beaujardiere arranged GEM data collection intervals. We thank J. Slavin, G. Siscoe, and W. J. Hughes for helpful discussions. We thank R. Smith for providing the Longyearbyen meridian scan photometer data used for confirmation of the Ny Ålesund results and K. Tsuruda for supplying the Geotail electric field data. We acknowledge E. Friis-Christensen, T. Rosenburg, R. Doe, W. J. Hughes, and V. Angelopoulos for submitted data and discussions at the GEM Workshops which influenced the research but were not directly used in this study. This work was supported in part by the U. S. Air Force Office of Scientific Research task 2311PL05, NSF grant ATM-9401629, and NASA grant NAGW 2627.

The Editor thanks V. A. Sergeev and M. B. Moldwin for their assistance in evaluating this paper.

References

Akasofu, S.-I., The development of the auroral substorm, *Planet. Space Sci., 12*, 273, 1964.

Angelopoulos, V., V. A. Sergeev, F. S. Mozer, K. Tsuruda, S. Kokubun, T. Yamamoto, R. Lepping, G. Reeves, and E. Friis-Christensen, Spontaneous substorm onset during a prolonged period of steady, southward interplanetary magnetic field, *J. Geophys. Res., 101*, 24583, 1996.

Baker, D. N., and R. L. McPherron, Extreme energetic particle decreases near geostationary orbit: A manifestation of current diversion within the inner plasma sheet, *J. Geophys. Res., 95*, 6591, 1990.

Baumjohann, W., Y. Kamide, and R. Nakamura, Substorms, storms, and the near-Earth tail, *J. Geomagn. Geoelectr., 48*, 177, 1996.

Belian, R. D., G. R. Gisler, T. Cayton, and R. Christensen, High-Z energetic particles at geosynchronous orbit during the great solar proton event series of October 1989, *J. Geophys. Res., 97*, 16,897, 1992.

Blanchard, G. T., L. R. Lyons, O. de la Beaujardiere, R. A. Doe, and M. Mendillo, Measurement of the magnetotail reconnection rate, *J. Geophys. Res., 101*, 15,265, 1996.

Caan, M. N., R. L. McPherron, and C. T. Russell, Substorm and interplanetary magnetic field effects on the geomagnetic tail lobes, *J. Geophys. Res., 80*, 191, 1975.

Craven, J. D., and L. A. Frank, Latitudinal motions of the aurora during substorms, *J. Geophys. Res., 92*, 4565, 1987.

de la Beaujardière, O., L. R. Lyons, J. M. Ruohoniemi, E. Friis-Christensen, C. Danielsen, F. J. Rich, and P. T. Newell, Quiet-time intensifications along the poleward auroral boundary near midnight, *J. Geophys. Res., 99*, 287, 1994.

Elphinstone, R. D., et al., Observations in the vicinity of substorm onset: Implications for the substorm process, *J. Geophys. Res., 100*, 7937, 1995.

Erickson, G. M., Substorm theories: United they stand, divided they fall, U. S. Natl. Rep. Int. Union Geod. Geophys. 1991-1994, *Rev. Geophys., 33*, 685, 1995.

Erickson, G. M., and R. A. Wolf, Is steady convection possible in the Earth's magnetotail, *Geophys. Res. Lett., 7*, 897, 1980.

Frank, L. A., W. R. Patterson, K. L. Ackerson, S. Kokubun, T. Yamamoto, D. H. Fairfield and R. P. Lepping, Observations of plasmas associated with the magnetic signature of a plasmoid in the distant magnetotail, *Geophys. Res. Lett., 21*, 2967, 1994.

Fujii, R., R. A. Hoffman, P. C. Anderson, J. D. Craven, M. Sugiura, L. A. Frank, and N. C. Maynard, Electrodynamic parameters in the nighttime sector during auroral substorms, *J. Geophys. Res., 99*, 6093, 1994.

Greenspan, M. E., P. B. Anderson, and J. M. Pelagatti, Characteristics of the thermal plasma monitor (SSIES) for the defense meteorological satellite program (DMSP) spacecraft S8 through S10, *Rep. AFGL-TR-86-0227*, Air Force Geophys. Lab., Hanscom Air Force Base, MA, 1986.

Hardy, D. A., L. K. Schmidt, M. S. Gussenhoven, F. J. Marshall, H. C. Yeh, T. L. Shumaker, A. Huber, and J. Pantazis, Precipitating electron and ion detectors (SSJ/4) for the block 5D/Flights 6-10 DMSP satellites: Calibration and data presentation, *Rep. AFGL-TR-84-0317*, Air Force Geophys. Lab., Hanscom Air Force Base, MA, 1984.

Hones, E. R., Jr., Substorm processes in the magnetotail: Comments on "On hot tenuous plasma, fireballs, and boundary layers in the Earth's magnetotail" by L. A. Frank, K. L. Ackerson, and R. P. Lepping, *J. Geophys. Res., 82*, 5633, 1977.

Hoshino, M., T. Mukai, A. Nishida, Y. Saito, T. Yamamoto, and S. Kokubun, Evidence of two active reconnection sites in the distant magnetotail, *J. Geomagn. Geoelectr., 48*, 515, 1996.

Hughes, W. J., and D. G. Sibeck, On the 3-dimensional structure of plasmoids, *Geophys. Res. Lett., 14*, 636, 1987.

Kaufmann, R. L., Substorm currents: Growth phase and onset, *J. Geophys. Res., 92*, 7471, 1987.

Kawano, H., et al., A flux rope followed by recurring encounters with travelling compression regions: Geotail observations, *Geophys. Res. Lett., 21*, 2891, 1994.

Kawano, H., et al., A quasi-stagnant plasmoid observed with Geotail on October 15, 1993, *J. Geomagn. Geoelectr., 48*, 525, 1996.

Kivelson, M. G., et al., The Galileo Earth encounter: Magnetometer and allied measurements, *J. Geophys. Res., 98*, 11,299, 1993.

Kokubun, S., T. Yamamoto, M. H. Acuña, K. Hayashi, K. Shiokawa, and H. Kawano, The Geotail magnetic field experiment, *J. Geomagn. Geoelectr., 46*, 7, 1994.

Lühr, H., H. S. Thürey, and N. Klöcker, The EISCAT magnetometer cross: Observational aspects, first results, *Geophys. Surv., 6*, 305, 1984.

Lyons, L. R., A new theory for magnetospheric substorms, *J. Geophys. Res., 100*, 19,069, 1995.

Machida, S., T. Mukai, Y. Saito, T. Obara, T. Yamamoto, A. Nishida, M. Hirahara, T. Terasawa, and S. Kokubun, Geotail low energy particle and magnetic field observations of a plasmoid at X_{GSM} = -142 R_E, *Geophys. Res. Lett., 21*, 2995, 1994.

Maynard, N. C., W. J. Burke, E. M. Basinska, G. M. Erickson, W. J. Hughes, H. J. Singer, A. G. Yahnin, D. A. Hardy, and F. S. Mozer, Dynamics of the inner magnetosphere near times of substorm onsets, *J. Geophys. Res., 101*, 7705, 1996.

McPherron, R. L., C. T. Russell, and M. P. Aubry, Satellite studies of magnetospheric substorms on August 15, 1968: Phenomenological models for substorms, *J. Geophys. Res., 78*, 3131, 1973.

Moldwin, M. B., and W. J. Hughes, Geomagnetic substorm association of plasmoids, *J. Geophys. Res., 98*, 81, 1993.

Mukai, T., S. Machida, Y. Saito, M. Hirahara, T. Erresawa, N. Kaya, T. Obara, M. Ejiri, and A. Nishida, The low energy particle (LEP) experiment onboard the Geotail satellite, *J. Geomagn. Geoelectr. 46*, 669, 1994.

Nagai, T., K. Takahashi, H. Kawano, T. Yamamoto, S. Kokubun, and A. Nishida, Initial Geotail survey of magnetic substorm signatures, *Geophys. Res. Lett., 21*, 2991, 1994.

Newell, P. T., W. J. Burke, C. -I. Meng, E. R. Sanchez, and M. E. Greenspan, Identification and observation of the plasma mantle at low altitudes. *J. Geophys. Res., 96*, 35, 1991.

Nishida, A., M. Scholer, T. Terasawa, S. J. Bame, G. Gloeckler, E. J. Smith, and R. D. Zwickl, Quasi-stagnant plasmoid in the middle tail: A new preexpansion phase phenomena, *J. Geophys. Res., 91*, 4245, 1986.

Nishida, A., T. Mukai, Y. Saito, T. Yamamoto, H. Hayakawa, K. Maezawa, S. Machida, T. Terezawa, S. Kokubun, and T. Nagai, Transition for slow to fast tailward flow in the distant plasma sheet, *Geophys. Res. Lett., 21*, 2939, 1994a.

Nishida, A., T. Yamamoto, K. Tsuruda, H. Hayakawa, A. Matsuoka, S. Kokubun, M. Nakamura, and H. Kawano, Classification of the tailward drifting magnetic structures in the distant tail, *Geophys. Res. Lett., 21*, 2947, 1994b.

Nishida, A., T. Mukai, T. Yamamoto, and Y. Saito, Geotail observation of magnetospheric convection in the distant tail at 200 R_E in quiet times, *J. Geophys. Res., 100*, 23,663, 1995.

Nishida, A., T. Mukai, T. Yamamoto, Y. Saito, and S. Kokubun, Magnetotail convection in geomagnetically active times: 1. Distance to neutral lines, *J. Geomagn. Geoelectr., 48*, 489, 1996.

Rostoker, G., J. C. Samson, F. Creutzberg, T. J. Hughes, D. R. McDiarmid, A. G. McNamara, A. V. Jones, D. D. Wallis, and L. L. Cogger, CANOPUS - A ground-based instrument array for remote sensing in the high latitude ionosphere during ISTP/GGs program, *Space Sci. Rev., 71*, 743,1994.

Sandholt, P. E., M. Lockwood, T. Oguti, S. W. H. Cowley, K. S. C. Freeman, B. Lybekk, A. Egeland, and D. M. Willis, Midday auroral breakup events and related energy and momentum transfer from the magnetosheath, *J. Geophys. Res., 95*, 1039, 1990.

Schindler, K., and J. Birn, On the generation of field-aligned flow at the boundary of the plasma sheet, *J. Geophys. Res., 92*, 99, 1987.

Sergeev, V. A., D. G. Mitchell, C. T. Russell, and D. J. Williams, Structure of the tail plasma/current sheet at $\sim 11\ R_E$ and its changes in the course of a substorm, *J. Geophys. Res., 98*, 17,345, 1993.

Singer, H. J., W. J. Hughes, P. F. Fougere, and D. J. Knecht, The localization of Pi 2 pulsations: Ground-satellite observations, *J. Geophys. Res., 88*, 7029, 1983.

Siscoe, G. L., Polar cap size and potential: A predicted relationship, *Geophys. Res. Lett., 9*, 672, 1982.

Siscoe, G. L., and W. D. Cummings, On the cause of geomagnetic bays, *Planet. Space Sci., 17*, 1765, 1969.

Slavin, J. A., R. P. Lepping, and D. N. Baker, IMP 8 observations of traveling compression regions: New evidence for near-Earth plasmoids and neutral lines, *Geophys. Res. Lett., 17*, 913, 1990.

Slavin, J. A., M. F. Smith, E. L. Mazur, D. N. Baker, E. W. Hones Jr., T. Iyemori, and E. W. Greenstadt, ISEE 3 observations of traveling compression regions in the Earth's magnetotail, *J. Geophys. Res., 98* 15,425, 1993.

Slavin, J. A., C. J Owen, M. M. Kuznetsova, and M. Hesse, ISEE 3 observations of plasmoids with flux rope magnetic topologies. *Geophys. Res. Lett., 22*, 2061, 1995.

Tsuruda, K., H. Hayakawa, M. Nakamura, T. Okada, A. Matsuka, F. S. Moser, and R. Schmidt, Electric field measurements on the Geotail satellite, *J. Geomagn. Geoelectr., 46*, 693, 1994.

Vasyliunas, V. M., Magnetic field line merging, *Rev. Geophys., 13*, 303, 1975.

W. J. Burke, Phillips Laboratory, 29 Randolph Road, Hanscom AFB, MA, 01731-3010. e-mail: burke@plh.af.mil

A. Egeland, B. Jacobsen, Department of Physics, University of Oslo, P. O. Box 1048 Blindern, N-0316 Oslo, Norway. e-mail: alv.egeland@fys.uio.no

G. M. Erickson, Center for Space Physics, Boston University, 725 Commonwealth Ave., Boston, MA, 02215. e-mail: erickson@buasta.bu.edu

S. Kokubun, Solar Terrestrial Environment Laboratory, Nagoya University, Toyokawa 441, Japan.

H. Lühr, GeoForschungsZentrum Potsdam, Telegrafenberg, D-14473 Potsdam, Germany. e-mail: HLuehr@gfz-Potsdam.de

N. C. Maynard and D. R. Weimer, Mission Research Corporation, One Tara Blvd., Suite 302, Nashua, NH, 03062. e-mail: nmaynard@mrcnh.com

T. Mukai, Institute of Space and Astronautical Science, 3-1-1 Yoshinodai, Sagamihara 229, Japan.

M. Nakamura, Department of Earth and Planetary Physics, University of Tokyo, Tokyo 113, Japan.

G. D. Reeves, Los Alamos National Laboratory, MS D438, Los Alamos, NM, 87545. e-mail: reeves@lanl.gov

J. C. Samson, Department of Physics, University of Alberta, Edmonton, T6G 2J1, Canada. e-mail: samson @space.ualberta.ca

T. Yamamoto, Institute of Space and Astronautical Science, Kanagawa 229, Japan.

(Received August 30, 1996; revised January 13, 1997; accepted January 30, 1997.)